sustainability

MDPI

Article

Dynamic Sensitivity of Footbridges: Modal Identification, Human-Induced Vibrations, and Emerging Solutions for Sustainable Design

Anna Banas [1,*], Izabela Drygala [2] and Dominika Ziaja [3]

[1] Department of Engineering Structures, Faculty of Civil and Environmental Engineering and EkoTech Center, Gdansk University of Technology, ul. Narutowicza 11/12, 80-233 Gdansk, Poland
[2] Faculty of Civil Engineering, Cracow University of Technology, 31-155 Cracow, Poland; izabela.drygala@pk.edu.pl
[3] Department of Structural Mechanics, Rzeszow University of Technology, al. Powstańców Warszawy 12, 35-029 Rzeszów, Poland; dziaja@prz.edu.pl
* Correspondence: anna.banas@pg.edu.pl

Abstract

Lightweight and slender footbridges exemplify sustainable, material-efficient infrastructure, yet their vibration performance is frequently governed by high dynamic sensitivity, which directly affects serviceability, user comfort, and structural durability. This paper provides a critical review of full-scale experimental investigations and validated finite element simulations addressing the dynamic behavior of various footbridges, focusing on the influence of structural typology, material solutions, and excitation characteristics on vibration-related performance within sustainability-driven design objectives. This article is organized into three core research themes: (1) standards and guidelines in bridge engineering practice, (2) dynamics of footbridges with special structural response to human-induced loading, including walking, running, crowd actions, and higher harmonic contributions, and (3) case studies, based on which the gaps in the current approach are formulated. Based on a synthesis of findings from leading research on structural dynamics and sustainable infrastructure, this paper highlights critical gaps in current vibration serviceability guidance for footbridges. Concluding remarks delineate the principal research challenges and formulate evidence-based, practical recommendations to enhance the resilience, vibration comfort compliance, and sustainability of future footbridge infrastructure.

Keywords: footbridges; dynamic sensitivity; human-induced vibrations; vibration serviceability; modal identification; operational modal analysis (OMA); GFRP footbridges; sustainable bridge design

Check for updates

Academic Editor: Byungik Chang

Received: 22 January 2026
Revised: 18 March 2026
Accepted: 25 March 2026
Published: 2 April 2026

Copyright: © 2026 by the authors. Licensee MDPI, Basel, Switzerland. This article is an open access article distributed under the terms and conditions of the Creative Commons Attribution (CC BY) license.

1. Introduction

Pedestrian bridges constitute a key element of urban and transportation infrastructure, providing safe and convenient passage over natural and man-made obstacles such as roads, railway lines, or rivers [1–4]. Contemporary trends in architectural and bridge engineering design promote slender, lightweight, and aesthetically pleasing structures, which align with the goals of sustainable development by minimizing material utilization [5–7]. Reduced structural mass directly contributes to lower embodied energy and reduced CO_2 emissions associated with material production, particularly in steel and concrete bridge structures. Consequently, lightweight footbridge solutions are often considered resource-efficient

infrastructure systems within life-cycle-based sustainability assessments. However, this lightness and slenderness make pedestrian bridges particularly susceptible to dynamic loadings, especially those induced by pedestrian traffic [8–10]. The issue of their dynamic sensitivity has become one of the most significant challenges in civil engineering, directly affecting user comfort, perceived safety, and, in extreme cases, the fatigue durability of the structure [2,11,12].

The conventional design and calculation approach, often limited to the simple criterion of avoiding resonance by ensuring that the fundamental natural frequency of the structure exceeds 5 Hz, has proven insufficient for many modern, flexible systems [13,14]. Vibrations induced by a single person walking, a group of pedestrians, running, or even vandalism may lead to excessive accelerations, even when the basic frequency criteria are met. This phenomenon is amplified by the possibility of step synchronization within a crowd, which has historically led to spectacular cases of excessive vibrations, such as the London Millennium Bridge [15].

Current design standards, such as Eurocode [16], SETRA [17], ISO 10137:2007 [18], and Minister of Infrastructure Regulation [19], include guidelines for evaluating vibration comfort; however, they often lack detailed recommendations for complex loading scenarios, including lateral vibrations, the influence of higher harmonics of pedestrian-induced forces, or kinematic effects generated by vehicle traffic beneath the bridge [20]. In response to these gaps, advanced pedestrian load models have been developed in the scientific literature, including force models describing time-dependent interaction forces, as well as more complex biodynamic models that consider the interaction between a pedestrian and the vibrating structure, e.g., the spring mass damper (SMD) and the inverted pendulum (IP) models [9,21,22]. Verification of these models and assessment of the actual structural behavior require precise in situ dynamic measurements carried out using techniques such as Experimental Modal Analysis (EMA) or Operational Modal Analysis (OMA) [23].

The recent literature on the dynamic behavior of lightweight footbridges reveals a fundamental inconsistency between numerical predictions, experimental observations, and current design practice [13,24–26]. This discrepancy arises primarily because numerical FE models usually represent idealized structural systems and therefore neglect several sources of additional energy dissipation observed in real structures. In practice, damping may be significantly influenced by friction in bearings, connections between structural and non-structural components, deck surfacing layers, and interaction effects between pedestrians and the vibrating structure. For preliminary design purposes, typical damping ratios reported in the literature for footbridges usually range between approximately 0.2–3.0% [17]. On the one hand, full-scale experimental studies on GFRP footbridges demonstrate that pedestrian presence may significantly alter the dynamic response of the structure, for example, by increasing effective damping. While some experimental investigations indicate that pedestrians can act as additional dynamic dampers under certain conditions [27], other full-scale tests clearly show that lightweight composite footbridges may experience acceleration levels exceeding accepted comfort limits despite compliance with conventional frequency-based criteria [24]. In contrast, a substantial body of recent research relies predominantly on increasingly sophisticated numerical models of pedestrian-induced loading, including probabilistic and fuzzy representations of gait variability and uncertainty [28,29]. Although these approaches offer valuable insights into sensitivity and risk assessment, they are rarely validated against comprehensive in situ measurements on real structures, particularly under realistic service conditions involving pedestrian traffic. Moreover, available experimental data often focus on modal properties derived from free vibration tests, while detailed measurements of acceleration response during actual use remain scarce. As a result, significant uncertainty persists regarding the reliability of existing assessment

methods and the true vibration performance of slender, sustainable footbridge solutions in service.

A novel aspect highlighted in this work is the need to design pedestrian bridges based on a comprehensive analysis of their dynamic response, rather than merely satisfying simplified frequency criteria. In this context, this study examines whether the frequency-based screening approaches adopted in current design standards reliably identify footbridges that are not susceptible to pedestrian-induced vibrations. In this context, the term conventional design refers to footbridges conceived within the traditional engineering paradigm, prior to pedestrian-induced vibrations being recognized as a critical serviceability issue. Such structures were primarily designed with emphasis on Ultimate Limit States (ULS) and static load combinations, where pedestrian loads were treated as uniformly distributed static actions. The reference to frequency criteria is therefore intended only to characterize the typical dynamic properties observed in these conventionally designed footbridges, and not to describe the analytical procedure adopted in the present study. It is emphasized that vibrations may accelerate material fatigue, thereby directly affecting the sustainable life cycle of the structure. Consequently, existing pedestrian bridges with high dynamic susceptibility should be included in dynamic structural health monitoring (SHM) programs to ensure their long-term reliability [30]. This article provides a critical review of the current state of knowledge, synthesizing results from experimental and numerical studies for a wide spectrum of bridges, including those constructed from traditional materials (steel and concrete) and innovative ones (Glass Fiber-Reinforced Polymer composites, GFRP).

The cases studied and discussed in this work draw on investigations carried out by the authors over the past fifteen years. None of these structures had previously been identified as critical according to the commonly accepted lateral frequency criterion in the 0.5–1 Hz range. However, the full-scale measurements revealed pronounced and, in some cases, disproportionate vibration responses relative to what would be expected based solely on frequency-based screening. In this context, the term refers not to an anomalous or "special" behavior, but to amplified acceleration levels resulting from specific combinations of modal characteristics, damping ratios, and excitation conditions, even when the fundamental frequency lies outside traditionally assumed critical bands. These findings highlight the limitations of relying exclusively on simplified frequency criteria when assessing vibration serviceability. The aim of the work is therefore to identify key parameters influencing dynamic sensitivity, highlight gaps in existing guidelines, and, based on this information, (1) formulate recommendations for designing more resilient, comfortable, and sustainable pedestrian bridge structures, and (2) indicate strategies for the maintenance of existing facilities exposed to dynamic loads close to the resonance frequency.

This article is organized into three core research themes: (1) standards and guidelines in bridge engineering practice (Section 2.1), (2) dynamics of footbridges with special structural response to human-induced loading, including walking, running, crowd actions, and higher harmonic contributions (Section 2.2), and (3) case studies (Sections 2.3 and 2.4), based on which the gaps in the current approach are formulated (Sections 3 and 4).

2. Materials and Methods

This work is based on research conducted by the authors between 2010 and 2025, complemented by a systematic review of the literature and a synthesis of their findings across a wide range of footbridge structures. The methodology encompasses three main pillars: (1) a review and critical assessment of modal identification methods and design standards, (2) the compilation and analytical evaluation of a reference database of footbridges, and (3) a concise presentation of selected case studies that illustrate key dynamic challenges.

2.1. Standards and Guidelines in Bridge Engineering Practice

Dynamic performance of pedestrian footbridges has long been recognized as a serviceability issue within engineering practice, yet only a limited number of design guidelines provide explicit procedures for assessing vibration comfort under pedestrian-induced loading. The most widely cited documents include the French Sétra [17] recommendations, the European HiVoSS guidelines [31], and the DoLFfHIV guide [32] dedicated to lightweight footbridges. In the first generation of the Eurocodes, provisions addressing pedestrian-induced vibrations were distributed between EN 1991-2:2003 [33], which defined dynamic load models for footbridges, and EN 1990:2002+A1:2005 [34], which specified comfort criteria in terms of limiting accelerations. Although these documents provided a regulatory framework, the recommendations were relatively general and did not explicitly address more complex loading scenarios highlighted in recent research. This approach has been recently updated and structurally reorganized in the second generation of Eurocodes (EN 1990:2023 [35] and EN 1991-2:2023 [36]), which introduce a harmonized system combining traffic classes, harmonic load models, and explicit comfort verification procedures for pedestrian-induced vibrations.

Despite differences in terminology, scope, and modeling philosophy, all these documents adopt a broadly similar, two-step approach to the dynamic assessment of footbridges. The initial step is to verify whether the structure's natural frequencies fall within predefined critical ranges associated with high resonance susceptibility. This screening procedure is based on the assumption that if the fundamental vertical and horizontal frequencies lie outside these intervals, the vibration response induced by pedestrian traffic is unlikely to reach objectionable levels, and no detailed dynamic analysis is required.

The critical frequency bands for both vertical and horizontal modes vary slightly across guidelines, but the general trends are consistent. For vertical vibrations, Sétra, HiVoSS, and DoLFfHIV [17,31,32] identify the range 1.7–2.1 Hz as the most sensitive to resonance, particularly under synchronized walking. Frequencies below 1.0 Hz or above 5.0 Hz are generally considered non-problematic. In the former EN 1990:2002+A1:2005 framework [34], a simplified verification rule was adopted, requiring dynamic assessment whenever the fundamental vertical frequency was below 5 Hz, without distinguishing specific high-risk resonance bands. More recently, EN 1990:2023 [35] introduces explicitly defined critical frequency ranges for different vibration directions, replacing the previous single-threshold approach. In particular, the critical range is specified as 1.25–2.3 Hz for vertical and longitudinal vibrations (with an extended consideration up to 4.6 Hz for particularly sensitive structures). For horizontal vibrations, the most critical frequencies typically lie between 0.5 and 1.1 Hz (Sétra) or 0.7 and 1.0 Hz (HiVoSS/DoLFfHIV). While EN 1990:2002+A1:2005 adopted a simplified verification limit of 2.5 Hz for lateral and torsional vibrations, EN 1990:2023 introduces an explicitly defined critical range of 0.5–1.2 Hz for these vibrations.

If a footbridge exhibits natural frequencies within these critical ranges, the guidelines require evaluating predicted or measured accelerations from walking, running, or other group activities. These acceleration levels are compared with comfort thresholds. Vibration perception is inherently subjective and depends on numerous factors, including the direction of motion, its duration, and the posture or activity of pedestrians. In EN 1990:2002+A1:2005, recommended acceleration limits were given as 0.7 m/s^2 for vertical vibrations and 0.2 m/s^2 for horizontal vibrations in normal service conditions, while a value of 0.4 m/s^2 was permitted for horizontal vibrations under crowd loading conditions. In EN 1990:2023 (Annex H), acceleration limits are defined through comfort levels (CL1–CL3), with vertical limits of 0.5 m/s^2, 1.0 m/s^2, and 2.5 m/s^2 and horizontal limits of 0.1 m/s^2, 0.3 m/s^2, and 0.8 m/s^2, depending on the selected design situation and associated traffic

class. These values closely correspond to the comfort classifications proposed in Sétra, HiVoSS, and DoLFfHIV, which distinguish between acceptable, noticeable, uncomfortable, and unacceptable vibration levels. In the vertical direction, these classification limits are generally set at 0.5 m/s^2, 1.0 m/s^2, and 2.5 m/s^2, with accelerations above 2.5 m/s^2 deemed unacceptable. For horizontal motion, even relatively small accelerations may trigger forced synchronization ("lock-in") effects; the limits proposed by these guidelines typically range from 0.1 to 0.15 m/s^2, while values above 0.8 m/s^2 are classified as unacceptable [17,31,32]. Although linear FE models are commonly used for estimating modal frequencies and global dynamic properties, it should be noted that in very slender structures, particularly cable-stayed footbridges, geometric nonlinearities and amplitude-dependent damping effects may influence the vibration response. In such cases, advanced nonlinear analyses may provide a more accurate representation of large-displacement dynamics and human–structure interaction effects.

A number of technical documents and research studies emphasize that footbridges exhibiting particularly low natural frequencies—especially below 3 Hz—require a detailed dynamic analysis, regardless of their expected traffic intensity [17,31,32]. In Poland, existing regulations require [19] a detailed dynamic analysis whenever the fundamental frequency of a footbridge is below 3 Hz, irrespective of the vibration direction, with explicit verification of both ultimate and serviceability limit states, as well as user comfort. However, the regulations do not specify which comfort criteria should be applied, leaving their selection to engineering judgment. In parallel, several standards provide general guidance on selecting representative pedestrian load scenarios. EN 1990:2002+A1:2005 proposes defining load cases based on anticipated traffic conditions, including approximately 8–15 pedestrians under normal operating conditions and significantly larger pedestrian flows during exceptional events such as public gatherings or choreographed activities. The UK National Annex NA.2 to EN 1991-2 [37] further introduces a classification system for newly designed footbridges, assigning specific pedestrian load models to each class, with all groups considered unsynchronized unless specific circumstances suggest otherwise. In the updated framework of EN 1990:2023 and EN 1991-2:2023, this scenario-based approach has been further systematized by formalizing the linkage between design situations, traffic classes, and associated comfort levels.

Although these standards and guidelines [17,31,32] provide representative dynamic load models and typical pedestrian group sizes, they do not define universally applicable criteria for determining the exact number of individuals or the duration of excitation required to trigger critical vibration states in a specific structure. Consequently, for structures with low natural frequencies, the responsibility for selecting appropriate excitation models, estimating realistic pedestrian group sizes, and defining action durations ultimately rests with the designer. This underscores the continued need for engineering judgment and comprehensive dynamic assessment addressing both serviceability and user comfort requirements.

2.2. Dynamic Modal Models: From Research Objectives to Engineering Implementation

Identification of modal models, including the estimation of natural frequencies, mode shapes, and associated damping ratios, constitutes a fundamental problem in structural dynamics and vibration-based assessment. In the case of footbridges, modal identification is crucial due to their pronounced dynamic sensitivity and susceptibility to human-induced excitation [38,39].

A range of identification techniques has been applied to such structures, with OMA being the most adopted approach. In OMA, modal parameters are extracted under ambient or operational loading conditions, without the need for direct measurement of excitation

forces. However, owing to the high flexibility of pedestrian bridges, the presence of pedestrians and the variability of operational loads may significantly influence the identified modal properties [24]. Consequently, different identification techniques exhibit varying levels of robustness and accuracy in estimating modal characteristics, particularly when comparing EMA and operational modal analysis. An essential aspect of modal identification is the validation and updating of numerical finite element (FE) models of the investigated structures [40]. Reliable FE model calibration enables accurate numerical simulations of dynamic behavior and supports subsequent analyses related to vibration serviceability, structural health monitoring, and design optimization.

From a general perspective, the identification of structural dynamic properties serves the following principal objectives: global dynamic performance assessment; finite element model validation and updating; detection and localization of structural damage; and estimation of the remaining service life of structures. In selected applications, such as proof load testing or vibration-based structural health monitoring under dynamic operational conditions, simplified identification procedures are often adopted to ensure computational efficiency and robustness of parameter estimation.

Due to the time and cost consumption of modal parameters identification based on real-structure experiment data, and the increasing availability of statistical analysis, modal parameters identification is being replaced with statistical models. This approach requires collecting a huge number of patterns (describing the structure's vibrations in time and/or frequency domain). In the case of damaged appearance, the trained model should indicate the significant differences between the new-possessed signal and the collected database.

Despite the recognized importance of modal identification for understanding the dynamic behavior of slender structures, the assessment of bridge dynamics in engineering practice is still predominantly governed by procedures associated with proof load testing. These procedures are regulated by technical guidelines and accreditation requirements that define a limited scope of dynamic measurements, primarily aimed at verifying structural stiffness and global response rather than providing a comprehensive dynamic characterization.

In the case of pedestrian footbridges, current practice in Poland is based on guidelines such as the former GDDKiA recommendations (2008/2011) [41] and the more recent WR-M-23 recommendations [42], as well as accreditation requirements specified by the Polish Center for Accreditation (PCA DAB-15 [43]). Although these documents formally recognize the need for dynamic testing, their scope remains deliberately simplified and does not extend to full modal identification.

According to WR-M-23, dynamic tests of pedestrian footbridges are required mainly to determine fundamental natural frequencies and extreme response quantities, such as peak displacements or accelerations of the span. When the first natural frequency exceeds 3 Hz, the dynamic assessment may be reduced to frequency identification only, without further analysis of vibration response or user comfort. Importantly, the guidelines do not require the identification of mode shapes, estimation of damping ratios, or systematic evaluation of acceleration response under realistic pedestrian loading scenarios. As a result, the dynamic sensitivity of footbridges—particularly under synchronized pedestrian excitation—may remain insufficiently characterized within mandatory proof load testing procedures.

A similar philosophy was adopted in the earlier GDDKiA recommendations (2008/2011), where dynamic testing was treated as a supplementary component of proof load testing. While these guidelines allowed determination of natural frequencies and damping through free vibration decay, they did not impose requirements for detailed modal analysis, operational modal testing, or comfort-based assessment criteria. Moreover, pedestrian-induced loading scenarios were not explicitly defined, and the primary objective of dynamic tests

was the verification of structural stiffness and conformity with design assumptions rather than the evaluation of serviceability under human-induced vibrations.

The limited scope of dynamic measurements is further reinforced by the current accreditation framework for laboratories performing proof load tests. The PCA DAB-15 document specifies that dynamic testing may consist of measuring displacements, strains, or accelerations as a function of time, with minimum sampling frequencies of 200 Hz for road bridges and 300 Hz for railway bridges. However, the accreditation requirements do not mandate modal identification, damping estimation, finite element model validation, or comfort assessment according to vibration perception criteria. For pedestrian footbridges, the prescribed excitation scenarios include group walking, running, jumping, and horizontal excitation at balustrades, yet the evaluation is restricted to extreme response values rather than modal properties or frequency-dependent behavior.

Even more stringent technical standards developed for railway bridges, including structures designed for high-speed traffic, follow a comparable approach [44]. While railway standards impose mandatory dynamic analyses and define allowable acceleration limits for structural safety and traffic performance, they likewise do not require experimental identification of mode shapes or damping during proof load testing. Dynamic verification is focused on compliance with prescribed response thresholds rather than on a comprehensive understanding of the system's modal characteristics.

Consequently, across pedestrian, road, and railway bridge engineering practice, proof load testing represents a form of limited dynamic assessment, in which only selected global response parameters are measured and interpreted. Although such an approach is sufficient for formal acceptance and regulatory compliance, it does not provide the information required to assess dynamic sensitivity, human–structure interaction, or vibration comfort—issues that are particularly critical for lightweight and slender footbridges. This gap between regulatory practice and research-oriented modal identification underscores the need for extended dynamic testing strategies that go beyond the minimum requirements of proof load testing and incorporate full-scale modal identification and response-based evaluation of pedestrian-induced vibrations.

The Polish regulatory framework was selected as a representative example of nationally implemented proof load testing procedures, as it combines Eurocode-based design principles, ISO vibration criteria, and a formal accreditation system for testing laboratories. The identified limitations are therefore not country-specific but are inherent to the proof load testing philosophy adopted in many European countries.

2.3. Footbridge Reference Dataset

2.3.1. Footbridge Description

To ensure clarity of analysis and facilitate the interpretation of results, the dataset was organized into four categories: (a) beam-type footbridges, (b) arch-type structures, (c) cable-stayed footbridges, and (d) footbridges constructed from composite materials.

The first group of representative structures comprises beam-type steel footbridges located in Poland, summarized in Figure 1. One of the investigated structures (Figure 1a) is a single-span steel pedestrian bridge located over Chwarznieńska Street in Gdynia [45], Poland. The structure provides pedestrian access across a two-lane urban roadway and is equipped with staircases and elevator shafts to ensure accessibility for users with reduced mobility. The footbridge has a span of 21.00 m and an overall deck width of approximately 5.0 m, with a clear usable width of about 3.75 m between balustrades. The superstructure consists of four longitudinal steel I-girders supporting an orthotropic steel deck. The structural depth varies slightly along the span, reaching approximately 0.55 m at the supports. The deck is stiffened by open longitudinal ribs and transverse beams. The

bridge is supported on elastomeric bearings placed on reinforced-concrete piers founded on deep foundations.



Figure 1. Selected beam-type footbridges. Structures located over: (**a**) the Chwarznieńska street, Gdynia, (**b**) the national road S7, Mogilany, and (**c**) the Łagiewnicka Route, Kraków.

The second investigated beam-type pedestrian footbridge is located in Mogilany [26], southern Poland, and crosses the national road S7 (Figure 1b). The structure consists of three spans: a central span with a length of 30 m and two lateral spans with a total length of 14 m. The deck is composed of composite steel girders connected to a concrete slab approximately 15 cm thick by means of 814 steel Nelson-type shear connectors with a diameter of 16 mm and a height of 100 mm. The connectors are arranged along the longitudinal direction with an average spacing of approximately 200 mm and organized into groups of two (114 connectors) and four (744 connectors). At the ends of the lateral spans, reinforced concrete blocks with embedded steel beams are provided. These blocks serve both as protection of the steel members against corrosion induced by soil exposure and as end supports for the lateral overhangs. Pot bearings are installed between the deck and the two reinforced concrete piers.

Another example of a beam-type footbridge considered in this study is a single-span steel–concrete composite pedestrian bridge located in Kraków, which provides pedestrian access beneath the Łagiewnicka Route [46], one of the most significant recent civil engineering projects in the city (Figure 1c). The footbridge spans 48.0 m between supports and is designed as a steel truss integrated with a reinforced concrete deck slab with a thickness varying from 14 to 20 cm. The steel components are fabricated from S355-grade steel, while the reinforced concrete elements are made of C30/37 concrete.

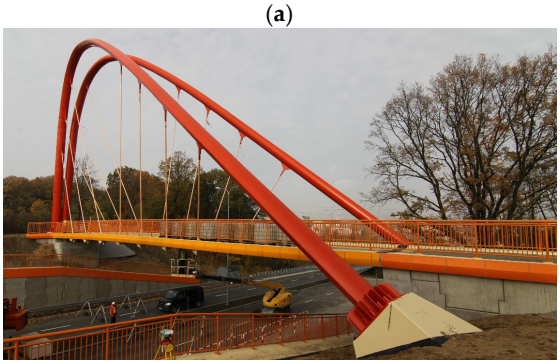
As the second group of representative structures, a set of arch-type footbridges located in Poland is presented. All arch-type structures are summarized in Figure 2. The first investigated structure (Figure 2a) is a steel–concrete arch footbridge located above the S8 expressway in Poland [47]. Completed in 2013, it provides pedestrian access between two vehicle service areas. The bridge has a total length of 50.0 m, a width of 4.5 m, and an overall height of approximately 7.5 m. The superstructure consists of two parallel steel arches supporting a reinforced-concrete deck through fourteen vertical steel hangers. Each arch is a circular hollow section with an outer diameter of 660.4 mm and a wall thickness of 20 mm. The arches are laterally braced by five tubular members of 323.9 mm diameter and 10 mm thickness. The deck cross-section consists of two longitudinal concrete beams of 0.60 m depth connected by a 0.20 m thick slab. The hangers are steel rods of 56 mm diameter. The structure is supported on pairs of elastomeric bearings at both abutments, with reinforced-concrete substructures founded on large-diameter piles. The second investigated structure (Figure 2b) is a steel–concrete footbridge located above the University Route in Bydgoszcz [47], Poland. Completed in 2013, the bridge has a total length of 34.40 m, a width of 4.5 m, and a structural height exceeding 20 m above the girder supports. The superstructure comprises a reinforced-concrete deck carried by two distinctive steel girders and fourteen steel hangers. The steel girders have a spatial triangular form, with a tear-shaped cross-section 720 mm high, 900 mm wide, and 20 mm thick. The deck is a reinforced-concrete slab of variable thickness, ranging from 0.18 m along the longitudinal axis to 0.45 m at the outer edges. The hangers are closed steel rods of 60 mm diameter. The girders are supported on three reinforced-concrete blocks founded on piles, while the deck platform rests on elastomeric bearings placed on abutments with footing-type foundations. The third investigated structure is the longest span P3 of the Kolibki footbridge [13], a steel arch–girder pedestrian and bicycle bridge located in Kolibki Park in Gdynia, Poland, spanning the Kolibki stream (Figure 2c). The structure has a total length of 51 m and a width of 4 m and is composed of four simply supported spans of 5.81 m, 11.62 m, 27.62 m, and 5.81 m, with a longitudinal inclination of approximately 1%. The main load-bearing system of span P3 consists of two parallel vertical arch–girders acting as a Vierendeel beam and supporting an orthotropic steel deck on both sides. Each girder comprises a straight longitudinal tube and a curved arch, both with an external diameter of 298.5 mm; the wall thickness is 12.5 mm near the supports and 10 mm at midspan. The orthotropic deck consists of a steel deck plate welded to longitudinal T-shaped ribs and transverse cross beams. The arch and straight beam are connected by 21 vertical tubular hangers. The system is welded throughout and is symmetric in the longitudinal direction, with slight transverse asymmetry near midspan. The deck is carried at both span ends by elastomeric bearings placed under the longitudinal beams. In the P3 span, the bearings rest on a reinforced-concrete pier consisting of two columns joined by a concrete cap, while the terminal spans are supported on one side on abutments with shallow foundations. The pier is founded on steel pipe piles with open bottoms.

The third group of representative structures includes cable-stayed footbridges located in Poland, summarized in Figure 3. The first structure is a steel–concrete composite cable-stayed footbridge with a total length of 120.00 m and a 3.00 m usable deck width (Figure 3a) [48]. It comprises three spans: a 60.00 m main span and two side spans of 25.50 m each. The deck consists of steel girders and a reinforced-concrete slab of 15–18 cm thickness, forming a grid of IPE360 longitudinal girders and IPE220 cross beams. The deck is suspended from two 11.80 m-high steel pylons (17° inclination) using Macalloy 460 bars of Ø64 mm. Cable lengths are: outer spans—28.00 m and 16.00 m; main span—30.00 m and 19.00 m. Four suspension points are used on the main span (spacing 12.00 m), while each side span is supported at a single point 13.50 m from the intermediate pier. Elastomeric

bearings connect the deck to the abutments, and all supports are founded on Ø100 cm reinforced-concrete piles. The second footbridge (Figure 3b), located over the DK-1 road in Częstochowa [49], is a two-span steel–concrete composite deck suspended from a pylon fixed into the central support. The central support consists of two reinforced-concrete piers connected by a transverse beam; the abutments follow the same structural scheme. The pylon is formed by two outward-inclined (8°) steel tubes filled with concrete. The deck comprises HEB 400 longitudinal girders and HEA 300 cross beams, except at hanger locations where Ø273 mm steel tubes are used. The longitudinal girder spacing is 2.80 m, and the slab thickness ranges from 0.17 to 0.20 m, compositely connected via shear studs. The deck is suspended in two planes using ASDO M42 cable systems, anchored to both the pylon and the deck through articulated fork connections.



(**a**)



(**b**)



(**c**)

Figure 2. Selected arch-type footbridges. Structures located over: (**a**) the S8 expressway, (**b**) the University Route in Bydgoszcz, and (**c**) the Kolibki stream.

The fourth group of representative structures comprises footbridges constructed from composite materials and located in Europe, summarized in Figure 4. The first composite footbridge (Figure 4a) is a GFRP structure located approximately 2 km from the city of Lleida in Spain [2]. Completed in October 2001, it provides a crossing over a roadway designed for the Madrid–Barcelona high-speed rail line. The bridge has a span of 38.00 m and is constructed entirely from pultruded GFRP profiles. The longitudinal modulus of elasticity ranges from 23 to 27 GPa, depending on the profile type. All joints are mechanically connected using stainless-steel brackets and bolts. The second structure (Figure 4b) is a simply supported GFRP footbridge with a U-shaped cross-section, inspired

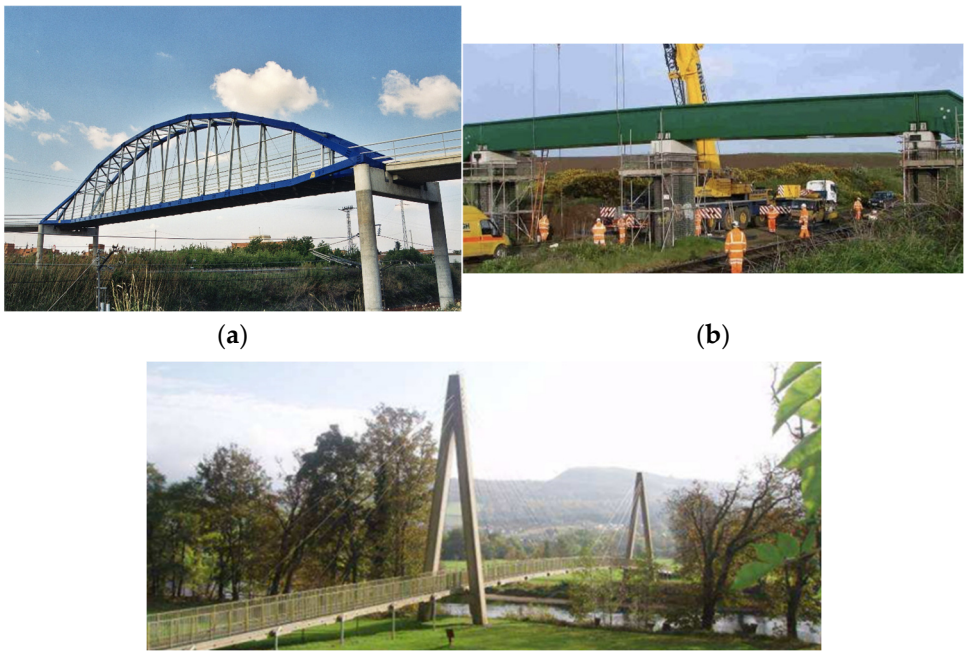
by the Bradkirk Bridge [2] erected in 2010 in Blackpool (Lancashire, UK). The bridge consists of two 12 m spans made of pultruded composite profiles forming a monolithic U-beam section. It serves as a pedestrian crossing over a railway line. The third example (Figure 4c) is an FRP cable-stayed footbridge located over the River Tay in Aberfeldy [5], Scotland. Constructed in 1992 as part of the Aberfeldy Golf Club infrastructure, the bridge has been the subject of previous detailed investigations addressing material characteristics, structural detailing, modal properties, and damping. These studies were primarily conducted to assess the condition of the structural components and verify their long-term performance.



(**a**)

(**b**)

Figure 3. Cable-stayed footbridges. Structures located over: (**a**) the Raba River in Lesser Poland, and (**b**) the DK-1 Route in Częstochowa [50].



(**a**) (**b**)

(**c**)

Figure 4. Composite materials footbridges: (**a**) Lleida, (**b**) Bradkirk, and (**c**) Aberfeldy.

2.3.2. Overview of the Adopted Methodology

The adopted research methodology was based on a comprehensive and integrated approach to the identification and assessment of the dynamic behavior of pedestrian footbridges, combining in situ experimental investigations, theoretical modeling, and numerical simulations. This study covered eleven pedestrian footbridges representing a wide range of structural systems, span lengths, and material configurations, providing a representative reference dataset. Out of the eleven investigated footbridges, eight were subjected to full-scale experimental testing, including modal identification under ambient and controlled excitation conditions; the corresponding experimental configurations, sensor layouts, and excitation types are summarized in Table 1.

Prior to the identification of dynamic parameters and the analysis of pedestrian-induced responses, all acceleration time histories recorded during the experimental campaign (including controlled excitation, ambient vibration, and pedestrian loading scenarios) were preprocessed to improve signal quality and ensure the robustness of the subsequent analyses. First, a basic quality control was performed by visually inspecting all recorded channels to detect sensor malfunction, clipping, unrealistic offsets, excessive noise, or acquisition artifacts; records affected by such issues were excluded from further processing. Next, constant offsets and/or linear trends were removed from the time series to suppress low-frequency drift. Finally, the detrended signals were filtered using an appropriate band-pass filter. The lower cut-off frequency was typically set in the range of 0.1–0.5 Hz to mitigate baseline drift, while the upper cut-off frequency was selected individually depending on the tested structure and the expected frequency range of interest, in order to remove high-frequency noise outside the relevant band. The resulting preprocessed signals were used as input for both the applied modal parameter identification techniques and the evaluation of vibration levels under pedestrian loading.

The primary objective of the experimental program was the identification of the fundamental modal parameters of the structures, including natural frequencies, mode shapes, and damping ratios. Depending on the structural characteristics and site-specific constraints, both output-only techniques based on ambient vibration measurements and input–output methods employing controlled excitation were applied. In selected cases, the tests were supplemented by pedestrian-induced loading scenarios, enabling evaluation of the dynamic response under realistic service conditions.

Experimental procedures were conducted using sensor layouts distributed along the decks, arches, and critical structural components such as hanger connections. Measurements included vertical and horizontal translational accelerations and, for selected structures, angular velocities, allowing for enhanced identification of complex modal behavior. Predominantly, MEMS-based sensors were employed, and data were acquired using synchronized multi-channel acquisition systems. Where the number of available channels was limited, multi-setup measurement strategies were adopted, with fixed reference sensors ensuring consistency between individual measurement configurations. The sensors used in the experimental campaign included MEMS accelerometers and gyroscopic sensors, namely LPY403AL and LIS344ALH (STMicroelectronics, Kirkop, Malta), TE 4332M3-002 and TE 4312M3-002 (Measurement Specialties, Hampton, VA, USA), 393B12 sensors (PCB Piezotronics, Depew, NY, USA), and IOLITEiw-3xMEMS-ACC acquisition systems (Dewesoft, Trbovlje, Slovenia).

Controlled excitation was introduced using electromechanical shakers, dynamic impact tests, and mass-based excitation devices, enabling extension of the excitation frequency range and assessment of the influence of excitation intensity and added mass on the identified modal parameters. Particular attention was paid to the interpretation of

results in cases where the applied excitation could affect the inherent dynamic properties of the structure.

Table 1. Experimental modal testing parameters for the reference dataset of the pedestrian footbridges. Adopted abbreviations: AV—Ambient Vibration.

Footbridge	Type of Sensor	Number of Configurations	Number of Measuring Points	Excitation Type
Over the Chwarznienska street in Gdynia [45]	TE 4332M3-002 TE 4312M3-002 MEMS gyroscopic sensors LPY403AL	1	24	Light exciter Heavy exciter AV
National road S7, Mogilany [26]	393B12 PCB Piezotronics	1	10 (3-axial)	AV
Łagiewnicka Route, Kraków [46]	IOLITEiw-3xMEMS-ACC	1	14 (3-axial)	AV
Over the S8 expressway [47]	LIS344ALH MEMS	1	10 vertical 2 horizontal	Impulse Light exciter
Over the University Route in Bydgoszcz [47]	LIS344ALH MEMS	1	10 vertical 3 horizontal	Impulse Light exciter
Over the Kolibki stream [13]	TE 4332M3-002 TE 4312M3-002 MEMS	6	47 vertical 45 horizontal	AV
Raba River in Lesser Poland [48]	393B12 PCB Piezotronics	1	6 (3-axial)	AV
DK-1 Route in Częstochowa [49]	393B12 PCB Piezotronics	1	4 (3-axial)	AV

Dynamic identification of pedestrian footbridges requires not only a reliable determination of modal parameters but also a systematic evaluation of structural response to human-induced loads. Pedestrians generate a broad spectrum of dynamic actions—walking, running, marching, and jumping—whose frequencies may interact with the natural frequencies of the structure, leading to resonance amplification, increased accelerations, and potential comfort issues. Full-scale tests remain the most representative and reliable source of data for both modal identification and serviceability assessment, as they capture realistic human–structure interaction effects that cannot be reproduced through simplified analytical models. A summary of the experimental pedestrian loading tests conducted on the eight investigated footbridges, including test types, number of participants, and synchronization conditions, is presented in Table 2.

Table 2. Summary of pedestrian loading tests conducted on the investigated arch-type footbridges.

Footbridge	Number of Tests	Type of Test	Number of Pedestrians	Synchronization
Over the Chwarznienska street in Gdynia [45]	18	walk, run, jump	1, 3, 6, 9	Synch/Free
National road S7, Mogilany [26]	21	walk, run, jump	1, 2, 3, 6	Synch/Free
Łagiewnicka Route, Kraków [46]	21	walk, run, jump	1, 2, 3, 6	Synch/Free
Over the S8 expressway [47]	23	walk, run, jump	6, 12	Synch/Free
Over the University Route in Bydgoszcz [47]	32	walk, run, jump	6, 9, 12	Synch/Free
Over the Kolibki stream [13]	23	walk with diff. freq.	1	Synch/Free
Raba River in Lesser Poland [48]	45	walk, run, jump	1, 2, 4, 6	Synch/Free
DK-1 Route in Częstochowa [49]	10	walk, run, jump	1, 2, 4, 9	Synch/Free

For a selected group of cable-stayed footbridges, a hybrid methodological framework was implemented, integrating experimental results with theoretical and numerical analyses. Simplified single-degree-of-freedom spring–mass–damper models incorporating pedestrian biodynamic effects were developed and calibrated using empirical data. These models were subsequently validated through finite element simulations, in which damping properties and boundary conditions were informed by the experimental findings. Dynamic

analyses focused on resonance-prone walking frequencies, and structural performance was evaluated using serviceability indicators such as peak acceleration and root mean square (RMS) values.

An additional group of structures, comprising footbridges constructed from composite materials, was investigated exclusively through numerical simulations. These analyses revealed specific dynamic characteristics, including a pronounced sensitivity to higher harmonics of pedestrian-induced loading when compared to footbridges built using conventional materials.

Overall, the adopted methodology, founded on the integration of experimental testing, theoretical modeling, and numerical simulation, provided a robust and consistent framework for the assessment of pedestrian-induced vibrations and the dynamic performance of vibration-sensitive footbridge structures.

2.4. Cases Obtained from Literature Studies

Parallel to the synthesis of results of one's examples of footbridges, careful studies of the literature were made. The literature review was conducted based on three primary sources: (1) materials gathered during the authors' prior scientific research, such as conference proceedings; (2) studies of local journals focusing on structure examples from the authors' home regions; and (3) a systematic search of the Scopus and Web of Science Core Collection databases performed between July and December 2026. The authors selected only high-quality papers from renowned journals or books available via institutional or open access (e.g., ScienceDirect or Wiley Online Library). The search, limited to publications released after 2000, utilized various combinations of keywords including 'footbridge', 'pedestrian bridge', 'vibration', 'dynamics', 'comfort class', 'dampers', and 'structural health monitoring'. From published articles, books, and conference materials, the footbridges were selected for which the dynamic parameters, obtained experimentally on real structures, were available. Altogether, the database with 47 samples documented in publications from the period between 2009 and 2026 was collected. It is described in detail in Section 3.2.

3. Results and Discussion

3.1. Parameter Identification of the Own Dataset Footbridges

The experimental investigations confirmed that slender pedestrian footbridges exhibit a wide spectrum of dynamic behaviors, strongly dependent on structural typology, mass distribution, and boundary conditions. The modal parameters of the investigated footbridges were identified using four experimental techniques, selected according to the applied excitation type and testing strategy. Peak Picking (PP) was applied to input–output data obtained from forced-vibration tests, whereas Frequency Domain Decomposition (FDD), Stochastic Subspace Identification (SSI-data), and Least-Squares Complex Exponential (LSCE) methods were used for the analysis of ambient vibration records. Numerical finite element models developed in SOFiSTiK versions from 2018 to 2025 or ANSYS 5.5 were subsequently calibrated and compared with the experimental results, showing a satisfactory agreement in terms of natural frequencies and identified mode shapes. Mode shape consistency between experimental and numerical results was assessed using the Modal Assurance Criterion (MAC), while damping ratios were estimated either from half-power bandwidth methods or directly from SSI- and LSCE-based identification. A summary of the experimentally identified modal parameters is presented in Tables 3–5. It should be noted that the mode labels reported in Tables 3–5 follow the notation adopted in the original source publications. Depending on the case study, letters such as V, H, T, L, DT, AL, etc., denote vertical, horizontal (lateral), tor-

sional, lateral, deck-related, or arch-related modes, respectively. Since the present work compiles previously published experimental results, the original nomenclature has been preserved to ensure consistency with the cited sources.

For beam-type footbridges (Table 3), fundamental vertical and torsional modes were identified with good consistency across the applied identification techniques (see Tables 5–9). The agreement between experimentally identified modal parameters and calibrated Finite Element Method (FEM) models was satisfactory, as reflected by low relative differences in natural frequencies and high MAC values (see Tables 5–9). For these comparatively simple structural systems, modal identification based on frequency values and mode shapes was generally unambiguous, providing a reliable basis for dynamic assessment. However, even for these comparatively simple systems, clusters of closely spaced modes were observed, which complicates unambiguous mode ordering based solely on frequency values. Another case that may lead to difficulties in distinguishing between modal shapes is the footbridge over Chwarznieńska Street in Gdynia, where groups of modes exhibiting similar deformation patterns on one side of the deck but different bending–torsional character were identified [45]. In such cases, the use of modal assurance criteria and mode shape interpretation was essential to avoid misclassification.

Table 3. Experimental dynamic identification results of the beam-type footbridges. Adopted abbreviations: IM—identification method; T—total mass of the superstructure; DPM—mass of the deck per meter of the footbridge length; RDF—relative difference in frequencies.

Footbridge	IM	Mode Number	Frequency [Hz]	Damping [%]	T [t]/DPM [t/mb]	FEM Model Comparison RDF [%]	MAC
Over the Chwarznienska street in Gdynia [45]	SSI FDD PP	T_1	2.90	0.4	30.962/1.47	0.69	0.989
		V_1	3.09	0.2		0.32	0.986
		VT_1	8.80	1.2		3.07	0.984
		V_2	10.41	0.8		2.21	0.958
		VT_2	14.80	0.6		13.11	0.956
		VT_3	18.27	2.3		2.19	0.927
		V_3	21.70	0.9		1.20	0.972
		VT_4	23.10	1.5		3.94	0.973
		V_4	28.79	0.8		5.80	0.841
		VT_5	38.59	5.4		0.96	0.951
National road S7, Mogilany [26]	SSI FDD	V	4.34	0.8	-	0.46	0.988
		T	4.80	0.7		3.96	0.964
		H	5.85	0.6		1.54	0.978
		T	10.50	0.4		1.81	0.878
		V	11.53	0.4		0.09	0.958
		V	19.87	0.3		5.18	0.982
Łagiewnicka Route, Kraków [46]	SSI LSCE	1V	2.03	1.20	-	1.48	0.96
		2H	3.62	1.81		3.87	0.93
		3V	5.76	0.59		3.47	0.95
		4T	6.03	0.35		8.13	0.92
		5V	11.75	0.36		0.85	0.96
		6T	13.06	0.58		6.36	0.89
		7V	15.71	0.30		0.06	0.95
		8T	18.71	0.28		5.33	0.88
		9V	20.79	0.62		0.82	0.94

For arch-type footbridges (Table 4), the complexity of modal identification was found to depend strongly on the structural configuration of the system. In the case of the footbridge over the S8 expressway [47], representing a relatively pure arch-supported structural form, modal identification was significantly more straightforward. Clear separation between successive modes was achieved, high MAC values were obtained, and the identified mode shapes were well distinguishable, resulting in a consistent experimental ordering of modes. In contrast, for more structurally complex systems, such as the footbridge over

the University Route in Bydgoszcz [47] and the Kolibki footbridge [13], difficulties in mode ordering were observed, particularly for horizontal and coupled bending–torsional modes. These observations indicate that while arch-type footbridges are often perceived as dynamically transparent systems, the introduction of refined, non-standard, or highly integrated structural forms may lead to complex dynamic behavior. For such structures, experimental investigations limited to a narrow excitation range or simplified testing procedures may not provide a reliable representation of the actual structural response under service conditions.

Table 4. Experimental dynamic identification results of the arch-type footbridges. Adopted abbreviations: IM—identification method; T—total mass of the superstructure; DPM—mass of the deck per meter of the footbridge length; RDF—relative difference in frequencies.

Footbridge	IM	Mode Number	Frequency [Hz]	Damping [%]	T [t]/DPM [t/mb]	FEM Model Comparison RDF [%]	MAC
Over the S8 expressway [47]	PP impulse	1–Vd1	1.76	4.2	311.18/ 5.10	3.5	0.99
		2–Vd2	3.23	0.4		−1.2	0.99
		3–Vd3	4.99	0.7		1.0	0.99
		4–Vd4	6.86	1.2		0.7	0.99
Over the University Route in Bydgoszcz [47]	PP Impulse/Exciter	1–B_Vd1	2.31	1.3	194.01/ 3.43	1.7	0.99/1.00
		2–B_La4	2.52	0.5		5.2	0.99/1.00
		3–B_Td1	4.77	2.1		3.8	0.99/-
		4–B_Td2	4.99	1.1		3.8	0.99/0.99
		5–B_Vd5	5.73	0.6		3.0	0.95/0.97
Over the Kolibki stream [13]	SSI	1–AL_1	4.27	2.186	38.14/ 1.07	27.21	0.768
		2–AL_2	5.04	0.144		35.67	0.993
		3–DV_1	5.28	0.332		0.53	0.992
		4–DV_2	6.21	0.923		11.18	0.98
		5–DT_1	7.21	2.036		-	-
		6–DT_2	8.05	0.619		17.9	0.837
		7–DT_3	8.99	0.482		2.03	0.965
		8–DT_4	11.51	1.592		-	-
		9–AL_3	12.01	0.450		13.15	0.945
		10–DT_5	12.66	4.291		-	-
		11–DV_3	14.12	0.334		5.2	0.958
		12–DV_4	17.7	0.604		3.11	0.537
		13–AL_4	19.06	0.203		13.06	0.931
		14–DT_6	19.62	1.094		−8.68	0.758

Cable-stayed footbridges (Table 5) exhibited comparatively low fundamental frequencies, often associated with vertical and horizontal global modes. Experimental–numerical agreement was generally at a good level. These results underline the importance of comprehensive modal identification when assessing dynamically sensitive systems with pronounced geometric and structural nonlinearity.

Across all investigated structures, identified damping ratios remained low, particularly for lightweight steel and composite systems, reinforcing the observation that limited inherent damping is a key contributor to elevated vibration susceptibility.

A recurring observation across the dataset is that footbridges with closely spaced modes—whether due to structural symmetry, arch–deck interaction, or cable-supported systems—are particularly challenging to assess using simplified criteria. In such cases, small uncertainties in identified frequencies or minor changes in operational conditions may lead to significant shifts in the dominant vibration response. This phenomenon may create a misleading perception of safety when assessment is based solely on frequency thresholds, or conversely, lead to overly conservative conclusions in structures that exhibit favorable damping or modal interaction effects.

Table 5. Experimental dynamic identification results of the cable-stayed footbridges. Adopted abbreviations: IM—identification method; T—total mass of the superstructure; DPM—mass of the deck per meter of the footbridge length; RDF—relative difference in frequencies.

Footbridge	IM	Mode Number	Frequency [Hz]	Damping [%]	T [t]/DPM [t/mb]	FEM Model Comparison RDF [%]	MAC
Raba River in Lesser Poland [48]	SSI LSCE	V1	1.91	1.46	-	1.57	0.97
		H1	2.35	1.26		0.43	0.95
		V2	2.57	1.23		0.39	0.95
		V3	3.80	1.19		1.32	0.91
		V4	4.35	0.53		0.46	0.74
DK-1 Route in Częstochowa [49]	FDD	1V	2.76	1.37	-	1.81	0.99
		2H	4.91	0.95		5.70	0.86
		3V	6.08	0.89		3.95	0.95

The Kolibki footbridge and selected arch-type and cable-stayed structures clearly illustrate that comprehensive modal identification, including mode shape analysis and damping estimation, is indispensable for a realistic evaluation of dynamic sensitivity.

Experimental pedestrian loading tests (Tables 6–8) demonstrated that, within the analyzed dataset, the vibration response was governed not only by the proximity of excitation frequencies to the identified natural modes but also by the specific combination of pedestrian activity, synchronization conditions, and modal characteristics of individual structures. The comparative analysis revealed that even for structures with similar fundamental frequencies, the measured acceleration levels varied significantly depending on whether pedestrian movement was free or synchronized. In particular, synchronized walking near the dominant vertical mode resulted in disproportionate amplification in selected typologies, highlighting the sensitivity of lightweight systems to controlled excitation scenarios beyond what could be inferred from frequency-based screening alone. Maximum acceleration values are reported for the participant numbers indicated in Table 2. Synchronized tests were conducted at frequencies close to the identified dominant mode. In this section, the dominant mode corresponds to the identified first vertical vibration mode of the structure, unless explicitly stated otherwise. In Tables 6–9, "Length" refers to the main span length, while "Mat." denotes the deck material, and f [Hz] denotes the identified natural bending frequency.

Table 6. Experimental results of pedestrian-induced load of the beam-type footbridges.

Footbridge	Length [m]	Mat.	f [Hz]	Type of Test	Max. Acc. [m/s^2]			
					Free		Sych.	
					V	H	V	H
Over the Chwarznienska street in Gdynia [45]	21.00	Steel	2.90	Walk	1.29	0.02	2.55	0.05
				Run	-	-	1.00	0.04
				Jump	-	-	3.61	0.05
National road S7, Mogilany [26]	30.00	RC	4.34	Walk	-	-	0.03	0.41
				Run			0.02	0.11
				Jump	-	-	0.08	0.68
Łagiewnicka Route, Kraków [46]	48.00	RC	2.03	Walk	1.02	0.04	2.36	0.12
				Run	0.47	0.05	0.98	0.06

It should be emphasized that running, jumping, and forced synchronization scenarios were included primarily as diagnostic loading cases rather than as direct comfort-based assessment conditions. These activities are not representative of typical service conditions and should therefore not be interpreted as standard vibration comfort checks. Instead,

they provide additional insight into resonance potential, modal participation, and the upper range of dynamic response. Although such loading scenarios are not intended for vibration comfort evaluation, they may still be structurally relevant in the context of dynamically sensitive footbridges. Occasional higher-amplitude pedestrian excitations can lead to increased stress fluctuations in selected structural components. From a long-term perspective, such effects may contribute to fatigue demand and therefore warrant consideration when interpreting the broader structural performance of the system.

Table 7. Experimental results of pedestrian-induced load of the arch-type footbridges.

Footbridge	Length [m]	Mat.	f [Hz]	Type of Test	Max. Acc. [m/s^2]			
					Free		Sych.	
					V	H	V	H
Over the S8 expressway [47]	50.00	RC	1.76	Walk	0.17	0.01	0.32	0.02
				Run	0.20	0.01	0.53	0.02
				Jump	-	-	0.48	0.03
Over the University Route in Bydgoszcz [47]	34.40	RC	2.31	Walk	0.09	0.02	1.84	0.24
				Run	0.48	0.06	0.70	0.13
				Jump	-	-	2.23	0.37
Over the Kolibki stream [13]	27.62	Steel	5.28	Walk	0.67	0.05	1.01	0.98

Table 8. Experimental results of pedestrian-induced load of the cable-stayed footbridges.

Footbridge	Length [m]	Mat.	f [Hz]	Type of Test	Max. Acc. [m/s^2]			
					Free		Sych.	
					V	H	V	H
Raba River in Lesser Poland [48]	60.00	RC	1.91	Walk	0.14	-	0.56	-
DK-1 Route in Częstochowa [49]	25.80	RC	2.7	Walk	0.29	-	2.102	-
				Run	0.93	-	2.38	-
				Jump	1.9	-	-	-

Table 9. Numerical results of pedestrian-induced load of the composite materials footbridges.

Footbridge	Structural Type	Main Span [m]	f [Hz]	Resonance Risk Level	Max. Acc. [m/s^2]–V	Vibration Comfort Level (SÉTRA)	Damping Ratio %
Lleida [2]	Double-tied arch	38.00	2.68	Medium	0.52	Mean	2.5
Bradkirk [2]	Simply supported U-beam	12.00	5.71	Negligible	0.49	Maximum	2.5
Aberfeldy [5]	Cable-stayed	31.50	1.64	Maximum	3.66	Uncomfortable	1.5

For some footbridges, particularly those with closely spaced modes or mixed vertical–torsional behavior, pedestrian-induced tests highlighted the limitations of associating a single "dominant frequency" with vibration risk. Even when the identified fundamental frequency appeared to lie outside traditionally critical ranges, higher modes or combined modal effects could still produce elevated accelerations under specific excitation conditions.

Numerical analyses of composite footbridges (Table 9) revealed a distinct dynamic behavior compared to traditional steel and concrete structures. Despite relatively low mass and favorable static performance, these systems exhibited increased sensitivity to higher harmonics of pedestrian-induced loading. Low damping ratios and reduced mass amplify acceleration response, particularly in resonance-prone frequency ranges. As a result, even moderate pedestrian excitation may lead to vibration comfort levels classified as uncomfortable according to SÉTRA criteria.

Overall, the results demonstrate that pedestrian footbridge dynamics cannot be reliably assessed using frequency-based criteria alone. Experimental identification shows that modal proximity, mode shape characteristics, damping variability, and human–structure interaction effects jointly govern vibration performance. The presented dataset confirms that full-scale testing and integrated interpretation of modal and response-based results are essential for identifying potentially critical dynamic behavior and for informing both design and assessment of sustainable, slender pedestrian bridge structures.

While the identified dynamic responses across a wide range of structural typologies reveal critical modal sensitivities, a key observation is the limited implementation of sustainable, damping-enhancing design strategies in existing footbridges. The results underscore that emerging solutions, such as composite materials (e.g., GFRP decks), advanced passive damping systems, and pedestrian-informed biodynamic models, are still largely underrepresented in practice. However, the efficiency of these mitigation strategies strongly depends on the specific structural configuration, vibration modes, and operational conditions of a given footbridge. In addition, such solutions are typically associated with significant installation costs that are highly project-specific and therefore difficult to generalize or compare directly across different case studies. It should be clearly stated that the present study does not incorporate passive damping systems or pedestrian-informed biodynamic models within the analyzed case studies. These approaches are mentioned solely to indicate promising directions in footbridge design and modeling that may address the limitations identified in conventionally designed structures and mitigate dynamic sensitivity. This gap, repeatedly revealed through comparative performance metrics and comfort assessments, confirms the need for integrating sustainability-driven innovations not only at the material level but also in vibration control strategies. Such integration is essential to ensure long-term serviceability, structural resilience, and lifecycle performance in lightweight footbridge design.

It should also be noted that most finite element models used in footbridge dynamics are based on linear assumptions, which are generally sufficient for modal parameter estimation and preliminary vibration assessment, and are consistent with current design guidelines for footbridge vibration assessment ([36], Annex G). However, in very slender systems, particularly cable-stayed or suspension footbridges, geometric nonlinearities may influence the dynamic response under human-induced excitation and should be considered in advanced modeling approaches [51–54].

3.2. Dynamic Properties of the Cases from Literature Studies

Objects found in the literature were ordered according to the type of structure and, inside these groups, also according to the length of the main span, and shown in Table 10. As can be seen, the data are not uniform. The structures are made with different materials (except for the group of GFRP footbridges; however, in this group, the detailed material properties were not studied). The applied dynamic testing methods are varied and sometimes even unknown; a similar situation occurs in the case of the identification method, modal, and total mass, or damping. Although EN 1990:2002+A1:2005 adopted a simplified verification limit of 2.5 Hz for lateral and torsional vibrations, and the revised EN 1990:2023 introduces a critical frequency range of 0.5–1.2 Hz for these modes, the present study focuses only on vertical and lateral vibrations reported in the analyzed literature sources.

This decision results from the fact that the majority of published experimental studies on footbridge dynamics report modal frequencies and serviceability indicators primarily for vertical and lateral (much less frequently) responses, which are directly related to pedestrian comfort criteria. Information on torsional vibrations is significantly less frequently reported

and often appears only as higher-order modes or coupled bending–torsional modes without dedicated comfort evaluation.

Consequently, to ensure consistency and comparability between the analyzed case studies, the present review limits the discussion to vertical and lateral vibration characteristics.

The results from human-excited vibration tests were available only for 15 of the 48 discussed objects. They are collected in Table 11. What is worth noticing is the lack of replicability of loading scenarios. It is an evident gap in testing requirements. The presented results, in the form of the maximum registered acceleration during the test, were caused by a varied number of pedestrians exciting the structure. In the case of availability of acceleration registered for a varied number of pedestrians, e.g., for a synchronized walk for groups of 6/11/28 people, their values are spaced using the '/' sign. The number of pedestrians alone is not sufficient for comparative studies between different objects; consideration of their mass in relation to the tested object would seem more important, but this type of data is rarity.

The analyzed case studies originate from a broad range of European and non-European countries; detailed geographical information can be retrieved from the cited references provided for each object in Tables 10 and 11.

In Tables 10 and 11, f [Hz] denotes the identified natural frequency. All reported frequencies refer to the fundamental vibration mode of the main span. When two values are separated by the symbol "/", the lowest identified frequency is given first. The symbols H and V indicate that horizontal and vertical mode shapes were reported, respectively. The torsional modes were not considered. The symbol ζ [%] denotes the modal damping ratio, while *M* and *T* represent the modal mass and total mass, respectively. In the tables, "Length" refers to the main span length, while "Mat." denotes the deck material, and the NoM means the number of mode shapes. The symbol N_{ped} denotes the maximum number of pedestrians involved in the test, while ToT indicates the type of pedestrian-induced excitation applied during the measurements, and the HC means half-crouching. The abbreviation N/A indicates that the data were not available, and OF denotes that only the first flexural mode was determined (for these cases, if two values of identified frequencies are given, it is the result of two applied excitation methods). The following material abbreviations are used: RC—reinforced concrete; S–C—steel–concrete composite; and Al + T_{glass}—aluminum alloy truss with a tempered glass deck.

Table 10. Dynamic identification of footbridges from the literature.

Footbridge	Length [m]	Mat.	Test Method	ID Method	Mass [kg]	Identified Values f [Hz]	ζ [%]	NoM
Beam-type footbridges								
Santos Station FB [55]	13.81	Steel	AVT	EFDD	N/A	H: 5.336 V: 13.340	0.35–0.75	4
N/A [21]	19.6	Al + T_{glass}	AVT + IT	PP	T: 36,430	H: 3.9551 V: 7.422	0.69	3
Nemšová [56]	24	Steel	AVT	OMA	N/A	V: 5.83 H: 9.24	1.0	7
Van Beethoven bridge [57]	30	Steel	N/A	N/A	M: 6300	V: 3.73 H: N/A	0.4	1
Eeklo [58]	42	Steel	AVT	SSI (ref.)	N/A	H: 1.71 V: 2.99	1.94 0.19	14
Podgorica [39]	78	Steel	AVT	PP	M: 58,000	V: 2.04 H: N/A	0.26	1

Table 10. *Cont.*

Footbridge	Length [m]	Mat.	Test Method	ID Method	Mass [kg]	Identified Values f [Hz]	Identified Values ζ [%]	NoM
Arch-type footbridges								
Anderlecht [58]	30	Steel	AVT	SSI (ref.)	N/A	H: 2.85 V: 3.24	0.45 0.31	10
Trabzon [59]	35	S-C	AVT	PP	N/A	V: 2.08 H: N/I	1.22	6
Modern Footbridge [60]	50.5	S-C	OMA	FDD	N/A	V: 2.25 H: 2.76	0.87 N/A	8
Butterfly-shaped Arch Bridge [61]	58	S-C	AVT	SSI	N/A	V: 1.247/ 2.084/4.105 H: N/A	0.6/0.3/0.2	6
Wetteren [58,62]	70.2	Steel	AVT	SSI (ref.)	N/A	H: 0.71 V: 3.74	2.12 0.76	10
A13 highway overpass in Bologna [63]	90	S-C	AVT	FDD SSI	N/A	V: 2.523 H: N/A	0.48	12
Pedro e Inês FB [38]	110	S-C	AVT	SSI_{COV}	N/A	V: 1.397 H: N/A	N/A	8
Cable-stayed footbridges								
Ninove [58,64]	36	Steel	AVT	SSI (ref.)	N/A	V: 2.97 H: 3.06	1.18 1.92	14
Nossa Senhora do Socorro Footbridge [65]	58	RC	OMA	PP FDD SSI_{UPC}	N/A	V: 1.63 H: N/A	N/A	4
Reep bridge Kortrijk [57]	61.5	Steel	N/A	N/A	M1: 47,000 M2: 33,000 M3: 19,000	V: 1.77/ 1.89/ 3.28 H: N/A	0.4/ 0.4/ 0.4	3
Rzeszów [66]	64	Steel/Wood	AVT	PP	N/A	H: 1.31 V: 1.96	6.1 5.4	5
Žarnovica–Lukavica Footbridge [67]	65	Steel	OMA	FDD	N/A	V: 1.23 H: N/A	N/A	9
Baker bridge [68]	72	S-C	AVT	SSI_{COV}	N/A	V: 0.93/2.0 H: N/A	0.22–0.55	6
Central Italy [69]	78	Wood	AVT	SSI-PC	N/A	V:1.16 H: 1.36	0.81 0.39	9
Umbria Gateway [70]	120	S-C	AVT	EFDD	N/A	V: 0.97 H: 1.67	N/A	8
Čelákovice [71]	156	RC	IH	PP	N/A	H: 0.58 V: 0.72	2.2 1.9	12
Suspension footbridges								
516 Arouca footbridge [72,73]	516	Steel	AVT	OMA	M1: 18,228 M2: 60,723	H: 0.113 V: 0.147	1.45 1.05	15
Composite materials footbridges								
Maldegem [27]	8.6	GFRP	HT + ET	PP	N/A	V: 4.54/4.44	4.10/9.00	OF
São Silvestre [74]	10.0	GFRP	AVT + IH	EFDD + $Poly_{-MAX}$	T: 3007	V: 8.39 H: N/A	2.47	4
Deurne [27]	10.0	GFRP	HT + ET	PP	N/A	V: 5.70/5.62	2.48/4.40	OF
Tremelo [27]	10.3	GFRP	HT + ET	PP	N/A	V: 5.19/5.36	3.20/5.02	OF
St. Mateus [75,76]	13.3	GFRP/ steel	IT	PP	T: 4608	V: 4.69 H: N/A	3.7 ± 0.053	2
St. Austell Bridge [14]	14.0	FRP	IH	GRFP	M: 2675 T: 5000	H: 6.48 V: 11.93	3.2 1.8	4
Galmaarden [27]	14.0	GFRP	HT + ET	PP	N/A	V: 5.19/5.27	3.21/4.43	OF
Dover Bridge [14]	14.5	FRP	IH	GRFP	M: 4870 T: 5500	V: 15.10 H: N/A	1.4	2

Table 10. *Cont.*

Footbridge	Length [m]	Mat.	Test Method	ID Method	Mass [kg]	Identified Values f [Hz]	ζ [%]	NoM
Delft Bridge B [14]	14.9	FRP	IH	GRFP	M: 3260 T: 6600	V: 6.12 H: N/A	7.9	4
Delft Bridge A [14]	15.0	FRP	IH	GRFP	M: 3161 T: 4500	V: 4.81 H: N/A	1.2	5
Puurs [27]	16.6	GFRP	HT + ET	PP	T: 8270	V: 3.81/3.79	0.07/2.61	OF
Parsons Bridge [14]	16.9	ACCS	IH	GRFP	M: 645 T: 1800	H: 4.30 V: 4.88	2.2 3.4	4
Ghent [27]	17.5	GFRP	HT + ET	PP	N/A	V: 4.91/4.78	0.12/6.68	OF
Bruges 2 [27]	17.6	GFRP	HT	PP	N/A	V: 5.21	0.04	OF
Bruges 1 [27]	18.0	GFRP	HT	PP	T: 22,000	V: 5.23	2.78	OF
Lille [27]	20.3	GFRP	HT + ET	PP	N/A	V: 4.81/4.81	0.06/0.71	OF
Prato Bridge [14]	25.0	FRP	AVT	SSI	T: 8000	H: 5.80 V: 7.46	1.8 2.6	7
Fiberline Bridge [77]	26.35	GFRP	IH	PP FDD	N/A	V: 4.35 H: N/A	0.52–2.77	7
Morstel [27]	29.2	GFRP	HT + ET	PP	T: 30,000	V: 3.91/3.90	0.08/0.64	OF
Halgavor Bridge [14]	47.0	FRP	AVT	SSI	T: 8600	V: 1.91 H: 2.12	2.3 0.8	10
Wilcott Bridge [14]	51.3	FRP	AVT	SSI	T: 31,000	V: 0.96 H: 1.08	2.5 0.3	9
Other								
circular footbridge in Rzeszów [25]	Ø40 m	Steel	AVT	MA	N/A	V:2.41/2.87 3.16/3.56 H: N/I	0.55/0.89 1.56/1.94	6
drawbridge across the Motlawa River in the city of Gdansk [78]	40.5	S-C	IT	ERA	N/A	V: 3.098 H: N/I	0.0343	4

Table 11. Results of pedestrian-induced load of the footbridges from the literature; adopted abbreviations: N/A—not available, N/I—not identified.

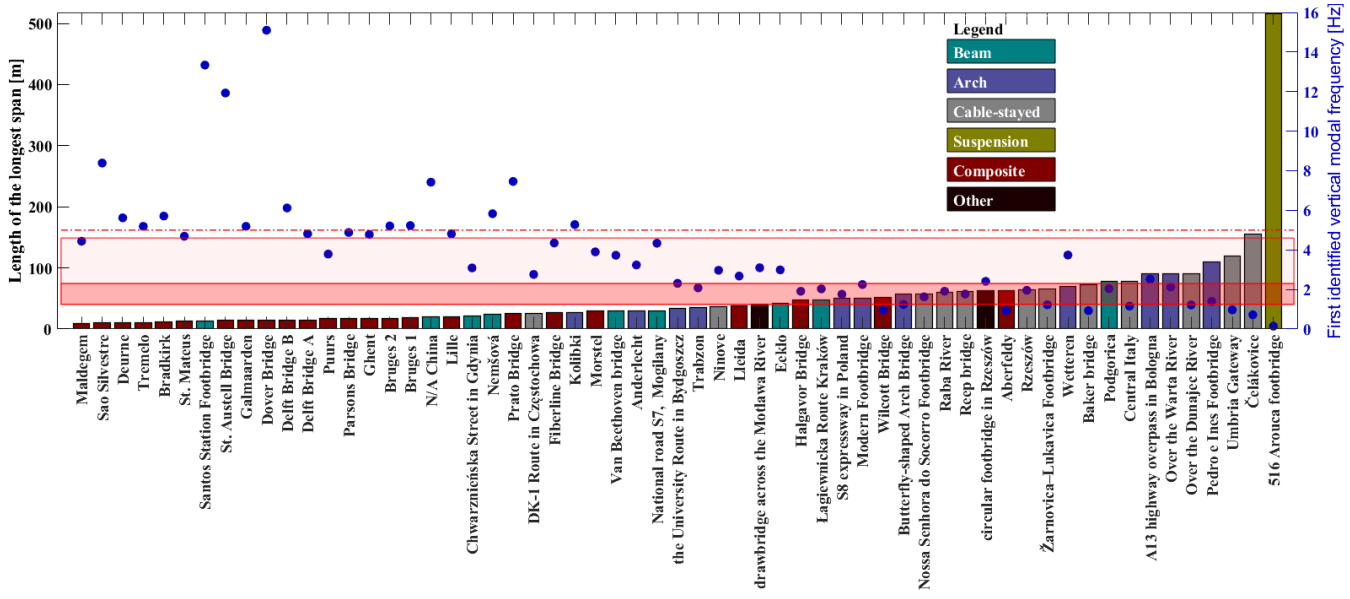
Footbridge	Length [m]	Mat.	f [Hz]	N_{ped}	ToT	Max. Acc. [m/s^2] Free V	Free H	Sych. V	Sych. H
N/A [21]	19.6	Al + T_{glass}	V: 7.422 H: 3.9551	14	Walk 2 Hz	N/A	N/A	1.09	0.426
Podgorica [39]	78	Steel	V: 2.04 Hz H: N/A	100	Walk	0.07–0.61	N/A	N/A	N/A
Over the Warta River (Poland) [6]	90	Steel	V: 2.13 H: N/A	10/20/30/40	Walk	0.34	0.12	0.59	0.26
					Run	0.89	0.44	1.35	0.41
					HC	N/A	N/A	1.28	0.41
Rzeszów [66]	64	Steel/Wood	H: 1.31 V: 1.96	1/6/15	Walk	0.26–1.05	0.11–0.55	0.33–1.98	0.15–0.67
					Run	0.53–1.59	0.15–3.20	1.22–2.78	0.48–2.29
				1/6	Jump	1.3	0.87–1.38	2.40–2.48	0.46–1.99
				6	Sway	N/A	N/A	0.8–0.93	1.0–2.8
Central Italy [69]	78	Wood	V: 1.16 H: 1.36	9	Walk	N/A	N/A	~0.40	~0.19
					Run	N/A	N/A	~1.80	~0.26
					Jump	N/A	N/A	~1.50	~0.17
Over the Dunajec River (Poland) [79]	90	Wood	V: 1.22/2.16 H: 1.13	12	Walk	0.21	N/A	2.20	N/A
					Run	1.11	N/A	3.14	N/A
					Run_{fast}	1.38	N/A	N/A	N/A
					HC	N/A	N/A	4.19	N/A

Table 11. *Cont.*

Footbridge	Length [m]	Mat.	f [Hz]	N_{ped}	ToT	Max. Acc. [m/s^2] Free V	Free H	Sych. V	Sych. H
516 Arouca footbridge [72,73]	516	Steel	V: 0.147 H: 0.113	34	Walk	>2.5	>0.8	N/A	N/A
Deurne [27]	10.0–10.0	GFRP	V: 5.70/5.62 H: N/A	6/11/28	Walk	0.654/ 0.599/ 0.767	N/A	N/A	N/A
					Run	1.438/ 1.698/ 2.056	N/A	N/A	N/A
Tremelo [27]	10.3	GFRP	V: 5.19/5.36 H: N/A	3/6/16	Walk	0.554/ 0.838/ 0.789	N/A	N/A	N/A
					Run	4.86/ 5.132/ 4.028	N/A	N/A	N/A
Puurs [27]	16.6	GFRP	V: 3.81/3.79 H: N/A	8/15/38	Walk	0.492/ 0.686/ 0.508	N/A	N/A	N/A
					Run	2.381/ 2.127/ 2.878	N/A	N/A	N/A
Fiberline Bridge (Denmark) [77]	26.35	Compsite GFRP	V: 4.35 H: N/A	2	Walk	0.60	N/A	0.80	N/A
					Run	1.67	N/A	2.07	N/A
					Jump	5.90	N/A	4.61	N/A
					Sway	3.11	N/A	1.91	N/A
St. Mateus [75,76]	13.3	GFRP/ Steel	V:4.69 H: N/A	1/3	Walk slow	0.28–0.48/ 0.6–0.62	N/A	-/ 0.73–0.75	N/A
				1/3/20	Walk norm	0.39–0.98/ 0.68–0.79/ 1.33–1.38	N/A	-/ 0.89–0.90/ -	N/A
				1/3	Walk fast	0.39–1.82/ 0.92–0.97	N/A	-/ 1.07–1.22	N/A
				1/3	Run	1.07–1.92/ 2.82–2.97	N/A	N/A	N/A
Ghent [27]	17.5	GFRP	V: 4.91/4.78 H: N/A	4/8/20	Walk	0.505/ 0.547/ 0.757	N/A	N/A	N/A
					Run	1.960/ 1.901/ 2.693	N/A	N/A	N/A
Morstel [27]	29.2	GFRP	V: 3.91/3.90 H: N/A	12/23/58	Walk	0.425/ 0.389/ 0.268	N/A	N/A	N/A
					Run	0.849/ 1.153/ 1.232	N/A	N/A	N/A
Circular footbridge in Rzeszów [25]	Ø40	Steel	V: 2.41 Hz and 2.87 Hz H: N/I	1/6/15/30/50	Walk	0.01/ 0.04/ 0.06/ 0.11/ 0.35	N/A	0.50/ 2.38/ 3.18 0.06/ 0.67/ 1.05	N/A
					Slow run	0.24/ 0.97/ 2.03/ 2.16/ 3.65	N/A	N/A	N/A
					Fast run	0.50/ 1.52/ 1.67	N/A	N/A	N/A
drawbridge across the Motlawa River in Gdansk [78]	40.5	Steel	V: 3.098 H: N/I	20	Walk	0.22	N/A	1.83	N/A
					Run	0.8	N/A	2.33	N/A
					Squad	N/A	N/A	3.08	N/A

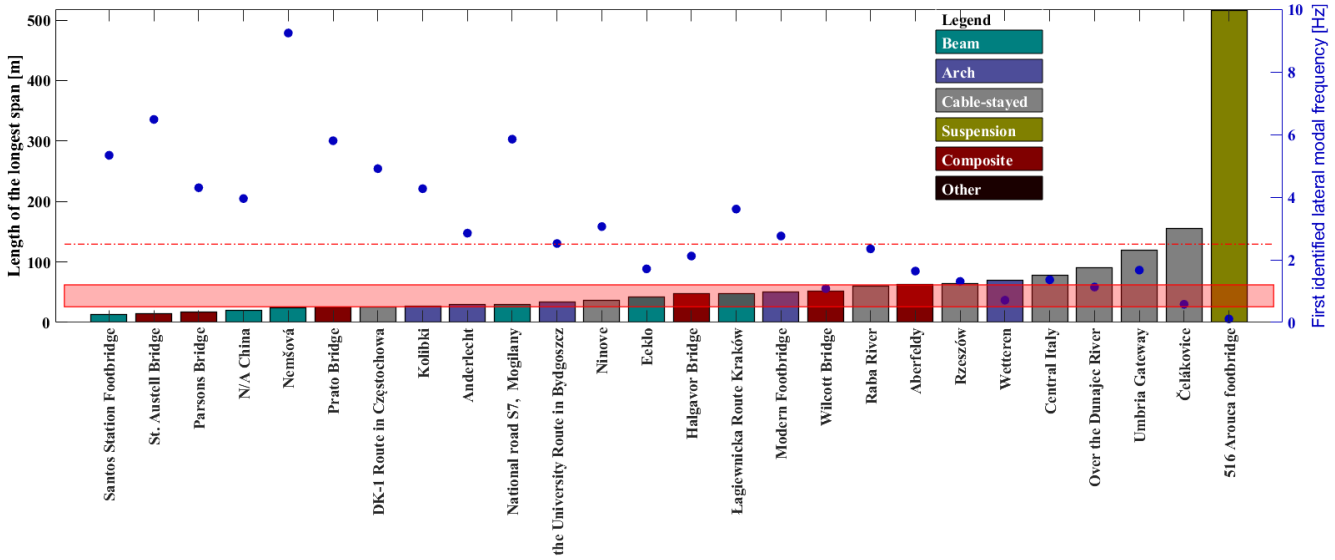
3.3. Analysis of Collected Cases

Despite the heterogeneity of the pattern set mentioned in Section 3.2, an attempt was made to determine the relationship between crucial parameters of the footbridges. For this purpose, the diagrams were prepared (Figure 5), in which the length of the main span (bar's height, scale on the y-axis on the left side), as well as the structure type (affiliation with the analyzed group described with the bar's color) and the first detected natural frequency (y-axis on the right side, blue dots), was shown for each of the analyzed bridges (from own examinations, as well as from the literature). Vertical and horizontal modes are shown in Figures 5a and 5b, respectively. Notably, lateral forms are documented for a much smaller number of footbridges in the literature. Each footbridge is a unique structure, so the comparison has rather a qualitative character, not a quantitative character. In the diagrams, red dotted–dashed lines were added. They show the suitable limitation according to the EN 1990:2002+A1:2005 [34] restrictions. The critical ranges according to the EN 1990:2023 [35] were marked using red rectangles. In Figure 5a, a light red rectangle was also added with the top magnitude equal to 4.6 Hz (with the application detailed in Section 2.1). What is interesting is that only 20 of the 59 objects, which is only 34%, fulfill the restrictions specified in [34] for vertical modes (Figure 6, bars on the right side of the red line—5 Hz limitation for the natural frequency of vibration in the vertical direction). Eleven of the analyzed objects (which is 19%) are included in the critical range for vertical vibration according to the EN 1990:2023 [35] (red rectangles in Figures 5a and 6), and after application of extended consideration up to 4.6 Hz for particularly sensitive structures (dark and light red rectangles together in Figures 5a and 6), even 46% (27 footbridges). Regarding lateral mode limitations, four out of the 26 available objects (15%) fall within the critical range for horizontal vibration according to EN 1990:2023 (indicated by the red rectangle in Figure 5b). Of course, the dataset consists of the selected group of objects (potentially problematic, described in the literature); some of them are older than the Eurocode regulation, but it indicates that the dynamic susceptibility problem refers not only to the newly designed objects but also to a large group of existing, aging facilities. In cases when the vibrations were not limited, it can be assumed that aging processes will progress faster than expected.



(**a**)

Figure 5. *Cont.*



(**b**)

Figure 5. The relation between the length of the main span, the type of structure, and (**a**) the first vertical and (**b**) first lateral detected natural frequency for the analyzed set of footbridges. Horizontal dotted–dashed line—the limitation for natural frequencies of vibration according to the EN 1990:2002+A1:2005 [34] restrictions (for vertical vibration—5 Hz; for lateral vibration—2.5 Hz); red rectangles—the critical ranges according to the EN 1990:2023 [35]; details in Section 2.1.

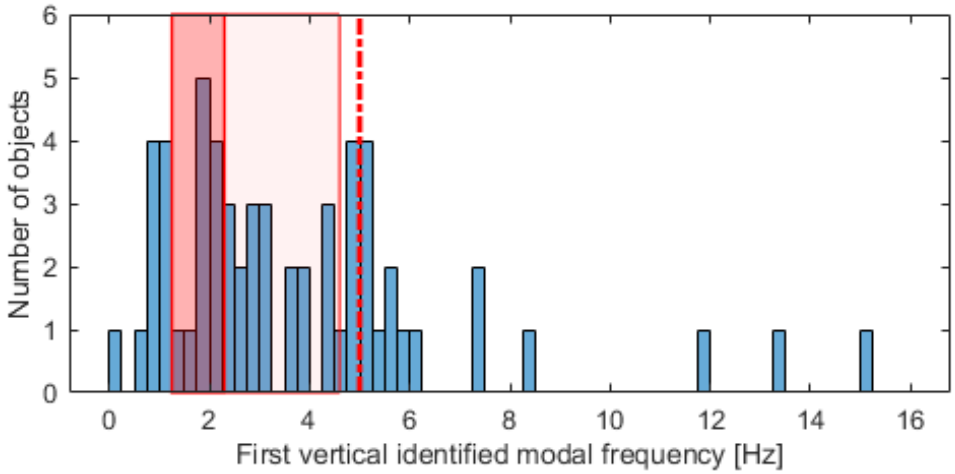


Figure 6. Histogram of the first detected vertical natural frequency for the analyzed set of footbridges. Red vertical line shows the limitation for natural frequencies of vibration in the vertical direction (5 Hz) according to the Eurocode EN 1990:2002+A1:2005 [34] restrictions; red rectangles—the critical ranges according to the EN 1990:2023 [35]; details in Section 2.1.

The analysis of the collected data was also conducted by the type of footbridge. Histograms in each category for both span length and first vertical natural frequency were presented as the diagonal plots on a matrix shown in Figure 7. The off-diagonal scatter plots show one of the analyzed parameters against the second one and vice versa. The nonlinear tendency observed in this figure was compared with simple conceptual models for the estimation of the first bending natural frequency of footbridges presented in [80]. The results are shown in Figure 8a for the whole set of analyzed footbridges and in Figure 8b for the narrowed set (without the structures with the lowest and the highest natural frequencies). As can be seen, the estimation curve 1 is the best simple model for most of the analyzed objects, especially for the composite footbridges. Prediction

of the first flexural frequency for composite bridges based on estimation curve 3 is statistically unjustified and, in many cases, overestimates, which in this task may cause problems. However, the best fit for the beam footbridges is estimation curve 3. Despite the estimation curves being directly dependent on the span length, the selection of the curve should be connected with the material and the type of footbridge. Usage of curve 2 leads to underestimation and curve 3 to overestimation of the first vertical natural frequency for the majority of cases. The estimation curves shown in Figure 8 facilitate early-stage predictions, allowing designers to assess whether a footbridge (with the considered span, shape, and made with selected materials) might experience vibration serviceability problems.

It should be noted that vibration performance assessments based on numerical predictions may be highly sensitive to modeling assumptions, particularly those related to boundary conditions and damping. Evidence from the literature [78] shows that modifying a key FE-model assumption associated with damping provision can markedly change both the modal properties and the predicted peak accelerations. For example, in a documented case study of a pedestrian bridge retrofitted with a viscous damping device, the first natural frequency increased from 1.64 Hz to 3.13 Hz, and the peak vertical acceleration under a representative pedestrian stream scenario decreased from 3.91 m/s^2 to 0.11 m/s^2. This illustrates that, beyond frequency-based screening, reliable comfort verification benefits from model calibration against measurements and/or sensitivity checks of the most influential parameters (e.g., support stiffness, connection stiffness, and assumed damping), especially for flexible structures.

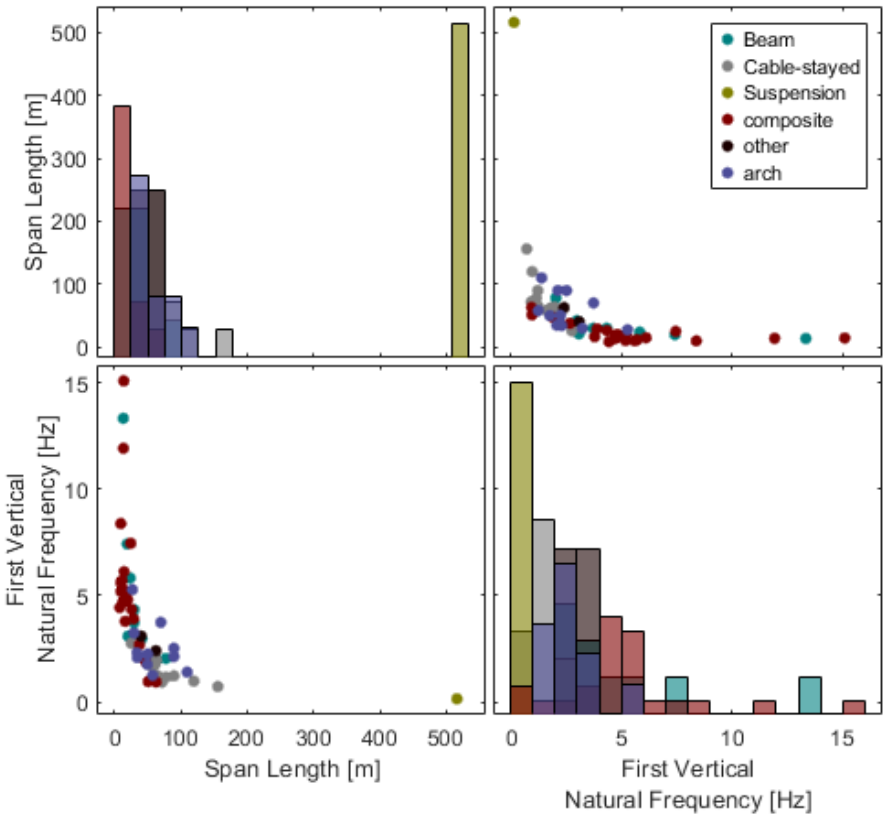


Figure 7. Matrix of scatter plots (off-diagonal) and histograms (diagonal plots) of the span length and first vertical natural frequencies for the analyzed footbridges, grouped by the considered categories.

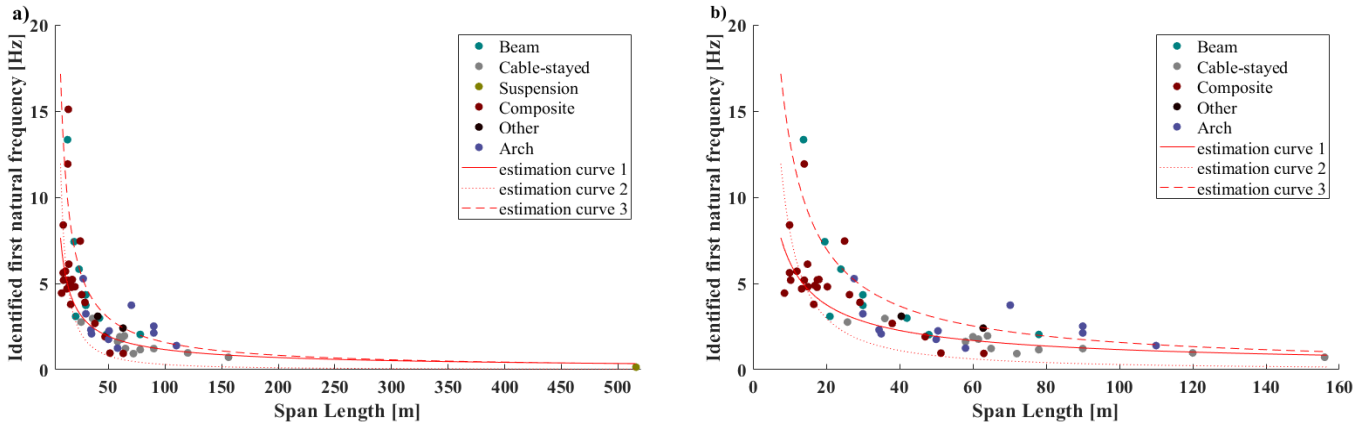


Figure 8. The relation between span length (L) and the first identified vertical natural frequency (f_1), considering the type of footbridge, in comparison with the estimation curves proposed in [80]; (**a**) for the whole set of analyzed footbridges, and (**b**) for a narrowed range (without objects with the lowest and the highest first natural frequency); estimation curve 1: $f_1 = 33.6L^{-0.73}$, estimation curve 2: $f_1 = 217L^{-1.431}$, and estimation curve 3: $f_1 = 112L^{-0.925}$.

4. Conclusions

This review of case studies conducted between 2010 and 2025 on the dynamic sensitivity of pedestrian footbridges leads to several key conclusions of both scientific and practical importance. Modern slender footbridges are confirmed to be highly susceptible to vibration, and their proper design requires an approach that extends well beyond simple frequency-based criteria. Ensuring adequate serviceability demands a comprehensive dynamic analysis that accounts for pedestrian-induced loading over a broad range of excitation frequencies, including higher harmonics capable of triggering resonance even in structures with seemingly safe natural frequencies. It should be emphasized that the frequency-based screening adopted in current design standards is intended solely as a preliminary classification stage to identify whether further dynamic verification is required, and not to predict vibration response or acceleration levels.

For footbridges classified as vibration-sensitive according to current design guidelines, the results confirm that detailed dynamic analysis and serviceability verification remain essential, as simplified frequency-based screening alone cannot reliably predict the actual vibration response under pedestrian loading. In this context, the role of frequency-based criteria is limited to indicating the need for further analysis, rather than providing a direct assessment of vibration performance. The comparative dataset also suggests that vibration susceptibility is particularly pronounced in lightweight systems with low mass and limited structural damping, such as composite or slender steel footbridges. The results indicate that reliable vibration assessment requires response-based analysis.

Reliable assessment of dynamic behavior and validation of FE models further necessitate advanced experimental investigations conducted in situ. Such studies should integrate diverse excitation techniques (impulse, harmonic, and operational modal analysis) together with high-quality measurement systems.

The analyzed case studies demonstrate that footbridges with similar fundamental frequencies may exhibit significantly different vibration responses depending on modal characteristics, damping properties, and pedestrian synchronization conditions. Importantly, the results also show that even structures classified as non-sensitive according to frequency-based screening may exhibit vibration levels exceeding comfort limits under realistic pedestrian loading conditions. These findings suggest that current design provisions may not fully capture certain aspects of the dynamic behavior of lightweight pedestrian

bridges, particularly with regard to higher harmonic excitation and kinematic interaction effects. This indicates the need for further refinement of design approaches to better reflect the complex dynamic response of contemporary pedestrian bridge structures. Existing codes insufficiently address the influence of higher harmonics and kinematic interactions, all of which play a significant role in lightweight and flexible structures. There is a clear and pressing need to update design provisions to better reflect the real dynamic behavior of contemporary pedestrian bridges.

Footbridges constructed from composite materials, such as GFRP, offer advantages in durability and weight reduction but exhibit very low damping and mass, making them especially susceptible to vibration problems. Their design requires careful attention and the application of refined dynamic analysis methods to ensure safe and comfortable performance.

From an engineering perspective, it is advisable that footbridges with higher dynamic susceptibility be equipped with supplemental damping systems or included in continuous or periodic structural health monitoring schemes. Such measures support long-term performance, user comfort, and effective management of operational risks.

The most practical implication of the present study is not the proposal of new numerical limits but the demonstration that frequency-based screening, while useful as an initial step, is not sufficient as a standalone assessment method and may lead to misleading conclusions. A structured response-based verification approach, including modal identification and synchronization-sensitive assessment, is therefore recommended for slender and lightweight footbridges.

In summary, achieving sustainable and reliable development of pedestrian footbridge infrastructure demands a holistic approach that integrates advanced numerical modeling, comprehensive experimental investigations, and design strategies that extend beyond the simplified frameworks of current standards.

Author Contributions: Conceptualization, I.D. and D.Z.; methodology, A.B. and I.D.; investigation, A.B., I.D. and D.Z.; resources, A.B., I.D. and D.Z.; data curation, A.B., I.D. and D.Z.; writing—original draft preparation, A.B., I.D. and D.Z.; writing—review and editing, A.B., I.D. and D.Z.; supervision, I.D.; project administration, A.B., I.D. and D.Z.; funding acquisition, A.B., I.D. and D.Z. All authors have read and agreed to the published version of the manuscript.

Funding: Part of this study was financially supported by Gdańsk University of Technology (grant DEC-26/1/2022/IDUB/I3b/Ag) under the ARGENTUM—'Excellence Initiative—Research University' program.

Institutional Review Board Statement: Not applicable.

Informed Consent Statement: Not applicable.

Data Availability Statement: No new data were created or analyzed in this study. Data sharing is not applicable.

Conflicts of Interest: The authors declare no conflicts of interest.

Abbreviations

The following abbreviations are used in this manuscript:

AVT	Ambient Vibration Testing
GFRP	Glass Fiber Reinforced Polymer
GRFP	Global Rational Fraction Polynomial
EMA	Experimental Modal Analysis
FDD	Frequency Domain Decomposition
FEM	Finite Element Method
FRF	Frequency Response Functions

IP	Inverted Pendulum
LCSE	Least Squares Complex Exponential
MAC	Modal Assurance Criteria
MARE	Mean Absolute Relative Error
MEMS	Micro-Electro-Mechanical-Systems
OMA	Operational Modal Analysis
PP	Peak Picking
PSD	Power Spectral Density
RD	Relative Difference
SHM	Structural Health Monitoring
SMD	Spring Mass Damper
SSI	Stochastic Subspace Identification
SVD	Singular Value Decomposition

References

1. Venuti, F.; Domaneschi, M.; Lizana, M.; Glisic, B. Finite Element Models of a Benchmark Footbridge. *Appl. Sci.* **2021**, *11*, 9024. [CrossRef]
2. Drygała, I.J.; Polak, M.A.; Dulińska, J.M. Vibration serviceability assessment of GFRP pedestrian bridges. *Eng. Struct.* **2019**, *184*, 176–185. [CrossRef]
3. Jiménez-Alonso, J.; Pérez-Aracil, J.; Hernández Díaz, A.M.; Sáez, A. Effect of Vinyl Flooring on the Modal Properties of a Steel Footbridge. *Appl. Sci.* **2019**, *9*, 1374. [CrossRef]
4. Li, Y.; Xiao, J.-X.; Li, C.; Li, J.-W. Investigations on the Influence of Pedestrians on the Buffeting of a Long-Span Suspension Footbridge. *Int. J. Steel Struct.* **2023**, *23*, 844–859. [CrossRef]
5. Drygała, I.J.; Dulińska, J.M.; Nisticò, N. Vibration serviceability of the Aberfeldy footbridge under various human-induced loadings. *Materials* **2023**, *16*, 2890. [CrossRef]
6. Hawryszków, P. Assessment of Pedestrian Comfort and Safety of Footbridges in Dynamic Conditions: Case Study of a Landmark Arch Footbridge. *Builder* **2021**, *285*, 78–82. [CrossRef]
7. Mulas, M.G.; Fortis, C.; Lastrico, G. Field-Testing and Serviceability Assessment of a Lively Footbridge. *J. Phys. Conf. Ser.* **2024**, *2647*, 122005. [CrossRef]
8. García-Diéguez, M.; Zapico-Valle, J.L. Sensitivity of the Vertical Response of Footbridges to the Frequency Variability of Crossing Pedestrians. *Vibration* **2018**, *1*, 290–311. [CrossRef]
9. Hawryszków, P.; Pimentel, R.; Silva, R.; Silva, F. Vertical Vibrations of Footbridges Due to Group Loading: Effect of Pedestrian–Structure Interaction. *Appl. Sci.* **2021**, *11*, 1355. [CrossRef]
10. Wang, Z.; Wen, J.; Kou, C.; Huo, H.; Chen, A.; Fan, B. Vertical human-structure interaction of a simply-supported steel-glass composite footbridge under both standing and moving pedestrians. *Structures* **2023**, *47*, 1212–1224. [CrossRef]
11. Ferreira, F.; Moutinho, C.; Cunha, Á.; Caetano, E. Use of semi-active tuned mass dampers to control footbridges subjected to synchronous lateral excitation. *J. Sound Vib.* **2019**, *446*, 176–194. [CrossRef]
12. Wang, L.; Zhou, Y.; Shi, W. Random crowd-induced vibration in footbridge and adaptive control using semi-active TMD including crowd-structure interaction. *Eng. Struct.* **2024**, *306*, 117839. [CrossRef]
13. Banas, A.; Nariswari, A.; Mulas, M.G. Modal Properties and Human Induced Vibration of an Arch Footbridge in Gdynia (PL). In *Proceedings of the Experimental Vibration Analysis for Civil Engineering Structures, Porto, Portugal, 2–4 July 2025*; Cunha, Á., Caetano, E., Eds.; Springer Nature: Cham, Switzerland, 2025; pp. 93–104. [CrossRef]
14. Wei, X.; Russell, J.; Živanović, S.; Mottram, J.T. Measured dynamic properties for FRP footbridges and their critical comparison against structures made of conventional construction materials. *Compos. Struct.* **2019**, *223*, 110956. [CrossRef]
15. Dallard, P.; Fitzpatrick, T.; Flint, A.; Low, A.; Smith, R.R.; Willford, M.; Roche, M. London Millennium Bridge: Pedestrian-Induced Lateral Vibration. *J. Bridge Eng.* **2001**, *6*, 412–417. [CrossRef]
16. *EN 1991*; Eurocode 1: Action on Structures. European Union: Brussels, Belgium, 2002.
17. Sétra/Afgc Sétra. *Technical Guide Footbridges Assessment of Vibrational Behaviour of Footbridges Under Pedestrian Loading*; Service d'études techniques des routes et autoroutes (SETRA): Paris, France, 2006.
18. *ISO 10137:2007*; Bases for Design of Structures—Serviceability of Buildings and Walkways Against Vibrations. International Organization for Standardization: Geneva, Switzerland, 2007.
19. *Rozporządzenie Ministra Infrastruktury z dnia 24 Czerwca 2022 r. w Sprawie Przepisów Techniczno-Budowlanych Dotyczących Dróg Publicznych (Dz.U.2022.1518) [pol. Minister of Infrastructure Regulation of June 24, 2022, on Technical and Construction Regulations Concerning Public Roads, Dz.U. 2022, Item 1518 (Poland)]*; Dziennik Ustaw Rzeczypospolitej Polskiej: Warsaw, Poland, 2022.

20. Kim, J.; Lynch, J.P. Experimental analysis of vehicle–bridge interaction using a wireless monitoring system and a two-stage system identification technique. *Mech. Syst. Signal Process.* **2012**, *28*, 3–19. [CrossRef]
21. Lu, C.; Xia, J.; Wang, X.; Wen, K.; Wang, Q.; Liu, Q. Analysis of Human-Induced Vibration Response and TLD Vibration Reduction of High Fundamental Frequency Aluminum Alloy Footbridge. *Structures* **2024**, *70*, 107579. [CrossRef]
22. Tubino, F.; Van Nimmen, K. Crowd-Induced Loading on Footbridges: Reliability of an Equivalent Spectral Model. *J. Phys. Conf. Ser.* **2024**, *2647*, 122006. [CrossRef]
23. Au, S.-K. Model validity and frequency band selection in operational modal analysis. *Mech. Syst. Signal Process.* **2016**, *81*, 339–359. [CrossRef]
24. Caprani, C.C.; Ngan, J.W.; Ahmadi, E.; Zhang, S.H.; Bai, Y.; Satasivam, S. Design, construction and performance of the Monash pultruded glass fibre-reinforced polymer footbridge. *Structures* **2023**, *51*, 970–984. [CrossRef]
25. Siwowski, T.; Janas, L. Numerical and experimental assessment of the dynamic behavior of a circular footbridge. In *Proceedings of the 9th International Conference on Structural Dynamics, EURODYN 2014, Porto, Portugal, 30 June–2 July 2014*; Cunha, A., Caetano, E., Ribeiro, P., Müller, G., Eds.; European Association for Structural Dynamics: Porto, Portugal, 2014.
26. Drygała, I.J.; Dulińska, J.M.; Nisticò, N.; Tatara, T. Impact of dynamic soil-structure interaction on performance of a single span footbridge with overhangs subjected to mining-induced shocks. *Materials* **2022**, *15*, 9084. [CrossRef]
27. Uyttersprot, J.; De Corte, W. Measured dynamic properties of web-core sandwich panel FRP composite footbridges and their relation to pedestrian comfort analysis. *Compos. Struct.* **2021**, *259*, 113236. [CrossRef]
28. Schweizer, M.; Fina, M.; Wagner, W.; Kasic, S.; Freitag, S. Uncertain pedestrian load modeling for structural vibration assessment in footbridge design. *Eng. Struct.* **2024**, *311*, 118070. [CrossRef]
29. Strobbe, S.; Van den Broeck, P.; De Corte, W.; Van Nimmen, K. Vibration serviceability assessment of footbridges: Extending the application range of current design guides. *Eng. Struct.* **2026**, *350*, 121814. [CrossRef]
30. Liew, J.P.; Rashidi, M.; Le, K.; Nazar, A.M.; Sorooshnia, E. Reviewing a Decade of Structural Health Monitoring in Footbridges: Advances, Challenges, and Future Directions. *Remote Sens.* **2025**, *17*, 2807. [CrossRef]
31. Feldmann, M. *Human-Induced Vibration of Steel Structures (HiVoss): Designing of Footbridges; Research Fund for Coal and Steel*; Publications Office of the European Union: Luxembourg, 2010.
32. Heinemeyer, C.; Butz, C.; Keil, A.; Schlaich, M.; Goldbeck, A.; Trometor, S.; Lukic, M.; Chabrolin, B.; Lemaire, A.; Martin, P.-O.; et al. *Design of Lightweight Footbridges for Human Induced Vibrations*; European Commission: Brussel, Belgium, 2009.
33. *EN 1991-2:2003*; Actions on Structures—Part 2: Traffic Loads on Bridges. European Union: Brussels, Belgium, 2003.
34. *EN 1990:2002+A1:2005*; Basis of Structural Design. European Union: Brussels, Belgium, 2005.
35. *EN 1990:2023*; Eurocode—Basis of Structural and Geotechnical Design. European Union: Brussels, Belgium, 2023.
36. *EN 1991-2:2023*; Eurocode 1—Actions on Structures—Part 2: Traffic Loads on Bridges and Other Civil Engineering Works. European Union: Brussels, Belgium, 2023.
37. *NA+A1:2020 to BS EN 1991-2:2003*; National Annex (Informative) to BS EN 1991-2:2003, Eurocode 1: Actions on Structures—Traffic Loads on Bridges. BSI Standards Limited: London, UK, 2020.
38. Hu, W.-H.; Moutinho, C.; Caetano, E.; Magalhães, F.; Cunha, Á. Continuous Dynamic Monitoring of a Lively Footbridge for Serviceability Assessment and Damage Detection. *Mech. Syst. Signal Process.* **2012**, *33*, 38–55. [CrossRef]
39. Govindan, R.; Lin, B.; Caprani, C.; Živanović, S. Footbridge Dynamics and Pedestrian Comfort: A Statistical Framework. In *Experimental Vibration Analysis for Civil Engineering Structures. EVACES 2025*; Lecture Notes in Civil Engineering; Cunha, Á., Caetano, E., Eds.; Springer: Cham, Switzerland, 2025; Volume 675. [CrossRef]
40. Drygała, I.J.; Dulińska, J.M. Full-scale experimental and numerical investigations on the modal parameters of a single-span steel-frame footbridge. *Symmetry* **2019**, *11*, 404. [CrossRef]
41. Łagoda, M.; Mazanek, M.; Olaszek, P. Zalecenia Dotyczące Wykonywania Badań pod Próbnym Obciążeniem Drogowych Obiektów Mostowych (2008/2011), Instytut Badawczy Dróg i Mostów, Warszawa 2008/2011 [pol. Recommendations for Carrying Out Load Tests on Road Bridge Structures (2008/2011), Road and Bridge Research Institute, Warsaw 2008/2011]. 2011. Available online: https://www.archiwum.gddkia.gov.pl/userfiles/articles/z/Zarzdzenia_Generalnego_2011/Z_A_L_E_C_E_N_I_A_probne_2011_tekst_ujednolicony.pdf (accessed on 24 March 2026).
42. Rymsza, J.; Olaszek, P. WR-M-23 Wytyczne Wykonywania Badań Drogowych Obiektów Mostowych pod Próbnym Obciążeniem. Wersja: 01, Rekomendował: Minister Infrastruktury w Dniu 2 Marca 2021 r. (DDP-4.0600.3.2021) [pol. Guidelines for Performing Road Tests of Bridge Structures Under Test Load. Version: 01, Recommended by: Minister of Infrastructure on March 2, 2021 (DDP-4.0600.3.2021)]. 2021. Available online: https://www.gov.pl/attachment/3da7d281-55dd-4451-945c-378f36f38865 (accessed on 24 March 2026).

43. Akredytacja Laboratoriów Badawczych Wykonujących Badania Obiektów Mostowych pod Próbnym Obciążeniem DAB-15 [Pol. Accreditation of Research Laboratories Performing Tests of Bridge Structures Under Test Load Dab-15], Polskie Centrum Akredytacji, Wydanie 2 Warszawa, 17.01.2024 r. 2024. Available online: https://www.pca.gov.pl/storage/file/core_files/2024/7/9/12809ab26cf5b8a72328bde8c19827ed/dab-15_2.pdf (accessed on 24 March 2026).
44. Standardy Techniczne Dotyczące Szczegółowych Warunków Technicznych dla Modernizacji lub Budowy linii Kolejowych do Prędkości Vmax $\leq$ 200 km/h (dla Taboru Konwencjonalnego)/250 km/h (dla Taboru z Wychylnym Pudłem), TOM III, Kolejowe Obiekty Inżynieryjne, Wersja 1.1, PKP Polskie Linie Kolejowe S.A. [pol. Technical Standards Concerning Detailed Technical Conditions for the Modernisation or Construction of Railway Lines Up to a Speed of Vmax $\leq$ 200 km/h (for Conventional Rolling Stock)/250 km/h (for Tilting Rolling Stock), VOLUME III, Railway Engineering Facilities, Version 1.1, PKP Polskie Linie Kolejowe S.A.]. 2014. Available online: https://www.plk-sa.pl/files/public/user_upload/pdf/Akty_prawne_i_przepisy/Standardy_techniczne/17.07.2019/Standardy_techniczne__2010_.zip (accessed on 24 March 2026).
45. Banas, A. Low-Cost Angular-Velocity Measurements for Sustainable Dynamic Identification of Pedestrian Footbridges: A Case Study of the Footbridge in Gdynia (Poland). *Sustainability* **2025**, *17*, 10456. [CrossRef]
46. Drygala, I.; Dulińska, J.; Jasińska, D.; Tatara, T.; Małecki, M.; Grabon, S.; Mesar, R. Dynamic Performance Analysis of a Single-Span Footbridge Supported by a Spatially Variable Truss. In *Experimental Vibration Analysis for Civil Engineering Structures. EVACES 2025*; Lecture Notes in Civil Engineering; Cunha, Á., Caetano, E., Eds.; Springer: Cham, Switzerland, 2025; Volume 675. [CrossRef]
47. Banas, A.; Jankowski, R. Experimental and Numerical Study on Dynamics of Two Footbridges with Different Shapes of Girders. *Appl. Sci.* **2020**, *10*, 4505. [CrossRef]
48. Bedon, C.; Drygała, I.J.; Dulińska, J.M.; Jasińska, D. Application of optimized spring– mass–damper pedestrian load models for vibration assessment of footbridges: Numerical and experimental investigation of a cable-stayed system. *Arch. Civ. Mech. Eng.* **2025**, *25*, 86. [CrossRef]
49. Drygala, I.J.; Dulinska, J.M.; Wazowski, M. Seismic Performance of a Cable-stayed Footbridge Using a Concrete Damage Plasticity Model. *Procedia Eng.* **2017**, *193*, 525–532. [CrossRef]
50. Michałowski, T. Cięgnowe przeprawy mostowe w Południowej Polsce, rozdział w Monografii Konstrukcje Mostowe, Metalowe i Drewniane—Kształtowanie, Ocena Stanu Technicznego Wybranych Elementów i Obiektów Budowlanych, Politechnika Krakowska, Kraków 2020. Available online: http://footbridge.pl/ (accessed on 6 December 2025).
51. Bin, Z.; Weiping, X.; Jian, X. Nonlinear Analysis for the Lateral Vibration of Footbridges Induced by Pedestrians. *J. Bridge Eng.* **2013**, *18*, 122–130. [CrossRef]
52. Deng, D.; Chen, G.; Chen, Z.; Zhang, X.; Lu, J. Study on Nonlinear Parametric Vibration of Footbridge Considering Time-Lag Effect. *IOP Conf. Ser. Mater. Sci. Eng.* **2019**, *490*, 032016. [CrossRef]
53. Yang, Z.; Jia, B.; Yan, Q.; Yu, X.; Zhao, Y. Nonlinear Stochastic Analysis of Footbridge Lateral Vibration Based on Probability Density Evolution Method. *Shock Vib.* **2019**, *2019*, 2606395. [CrossRef]
54. Dai, X.; Wei, X.; Tang, L.; Xue, Z.; Wu, Y. Vibration Suppression of Footbridges Using Nonlinear Vertical Absorbers. *Int. J. Mech. Sci.* **2026**, *313*, 111309. [CrossRef]
55. Xu, M.; Santos, L.O.; Campos, P. Assessment of Footbridge with Excessive Vibration. In *Experimental Vibration Analysis for Civil Engineering Structures. EVACES 2025*; Lecture Notes in Civil Engineering; Cunha, Á., Caetano, E., Eds.; Springer: Cham, Switzerland, 2025; Volume 675. [CrossRef]
56. Sykora, M.; Venglar, M. Assessment of the Steel Footbridge Using Ambient Vibrations. In *Experimental Vibration Analysis for Civil Engineering Structures. EVACES 2025*; Lecture Notes in Civil Engineering; Cunha, Á., Caetano, E., Eds.; Springer: Cham, Switzerland, 2025; Volume 675. [CrossRef]
57. Uyttebroeck, N.; Schevenels, M.; Lombaert, G. Design of TMDs for the vibration serviceability of footbridges using simultaneous sizing and topology optimization. *J. Sound Vib.* **2026**, *624*, 119504. [CrossRef]
58. Van Nimmen, K.; Lombaert, G.; De Roeck, G.; Van den Broeck, P. Vibration Serviceability of Footbridges: Evaluation of the Current Codes of Practice. *Eng. Struct.* **2014**, *59*, 448–461. [CrossRef]
59. Bayraktar, A.; Altunişik, A.C.; Sevim, B.; Türker, T. Modal Testing, Finite-Element Model Updating, and Dynamic Analysis of an Arch Type Steel Footbridge. *J. Perform. Constr. Facil.* **2009**, *23*, 81–89. [CrossRef]
60. Bohinc, U.; Franković, T.; Friedman, N.; Brank, B. Bayesian Structural Identification of a Modern Footbridge. In *Experimental Vibration Analysis for Civil Engineering Structures. EVACES 2025*; Lecture Notes in Civil Engineering; Cunha, Á., Caetano, E., Eds.; Springer: Cham, Switzerland, 2025; Volume 675. [CrossRef]
61. Wu, G.; Ren, W.-X.; Zhu, Y.-F.; Hussain, S.M. Static and dynamic evaluation of a butterfly-shaped concrete-filled steel tube arch bridge through numerical analysis and field tests. *Adv. Mech. Eng.* **2021**, *13*, 16878140211044671. [CrossRef]
62. Lourens, E.; Papadimitriou, C.; Gillijns, S.; Reynders, E.; De Roeck, G.; Lombaert, G. Joint input-response estimation for structural systems based on reduced-order models and vibration data from a limited number of sensors. *Mech. Syst. Signal Process.* **2012**, *29*, 310–327. [CrossRef]

63. Ubertini, F.; Gentile, C.; Materazzi, A.L. Automated Modal Identification in Operational Conditions and Its Application to Bridges. *Eng. Struct.* **2013**, *46*, 264–278. [CrossRef]
64. Lourens, E.-M.; Maes, K.; Van Nimmen, K.; Van den Broeck, P.; Guillaume, P.; De Roeck, G.; Lombaert, G. Multiple Localized Force Identification and Response Prediction on a Footbridge. PROCEEDINGS OF ISMA2012-USD2012. 2012. Available online: https://past.isma-isaac.be/isma2012/proceedings/toc/ (accessed on 9 March 2026).
65. Nunes, D.d.S.; Vital de Brito, J.L.; Doz, G.N. Dynamic Identification of a Cable-Stayed Footbridge Using a Low-Cost Data Acquisition System. *Rev. IBRACON Estrut. E Mater.* **2023**, *16*, e16610. [CrossRef]
66. Janas, L.; Basiaga, R. Badania dynamiczne podwieszonej kładki dla pieszych w Rzeszowie [pol. Dynamic Tests of the Suspended Pedestrian Bridge in Rzeszów]. *Zesz. Nauk. Politech. Rzeszowskiej. Bud. I Inżynieria Sr.* **2010**, *57*, 5–19.
67. Kortiš, J.; Daniel, Ľ.; Farbák, M.; Maliar, L.; Škarupa, M. Operational Modal Analysis of the Cablestayed Footbridge. *Civ. Environ. Eng.* **2017**, *13*, 92–98. [CrossRef]
68. Brownjohn, J.M.W.; Bocian, M.; Hester, D.; Quattrone, A.; Hudson, W.; Moore, D.; Goh, S.; Lim, M.S. Footbridge System Identification Using Wireless Inertial Measurement Units for Force and Response Measurements. *J. Sound Vib.* **2016**, *384*, 339–355. [CrossRef]
69. Nicoletti, V.; Quarchioni, S.; Tentella, L.; Martini, R.; Gara, F. Experimental Tests and Numerical Analyses for the Dynamic Characterization of a Steel and Wooden Cable-Stayed Footbridge. *Infrastructures* **2023**, *8*, 100. [CrossRef]
70. Pepi, C.; Gioffre', M.; Grigoriu, M.D. Parameters identification of cable stayed footbridges using Bayesian inference. *Meccanica* **2019**, *54*, 1403–1419. [CrossRef]
71. Šána, V.; Polák, M.; Plachý, T. A Dynamic Analysis of the Cable-Stayed Footbridge in Čelákovice Town. *Procedia Eng.* **2017**, *199*, 2877–2882. [CrossRef]
72. Tadeu, A.; Romero, A.; Dias, S.; Pedro, F.; Brett, M.; Serra, M.; Galvín, P.; Bandeira, F. Vibration serviceability assessment of the world's longest suspended footbridge in 2020. *Structures* **2022**, *44*, 457–475. [CrossRef]
73. Tadeu, A.; Romero, A.; Bandeira, F.; Pedro, F.; Dias, S.; Serra, M.; Brett, M.; Galvín, P. Theoretical and experimental analysis of the quasi-static and dynamic behaviour of the world's longest suspension footbridge in 2020. *Eng. Struct.* **2022**, *253*, 113830. [CrossRef]
74. Dacol, V.; Caetano, E.; Correia, J.R. Modal Identification and Damping Performance of a Full-Scale GFRP-SFRSCC Hybrid Footbridge. *Struct. Control Health Monit.* **2022**, *29*, e3137. [CrossRef]
75. Sá, M.F.; Guerreiro, L.; Gomes, A.M.; Correia, J.R.; Silvestre, N. Dynamic behaviour of a GFRP-steel hybrid pedestrian bridge in serviceability conditions. Part 1: Experimental study. *Thin-Walled Struct.* **2017**, *117*, 332–342. [CrossRef]
76. Sá, M.F.; Silvestre, N.; Correia, J.R.; Guerreiro, L.; Gomes, A.M. Dynamic behaviour of a GFRP-steel hybrid pedestrian bridge in serviceability conditions. Part 2: Numerical and analytical study. *Thin-Walled Struct.* **2017**, *118*, 113–123. [CrossRef]
77. Górski, P.; Tatara, M.; Stankiewicz, B. Vibration Serviceability of All-GFRP Cable-Stayed Footbridge under Various Service Excitations. *Measurement* **2021**, *183*, 109822. [CrossRef]
78. Żółtowski, K.; Banaś, A.; Binczyk, M.; Kalitowski, P. Control of the bridge span vibration with high coefficient passive damper. Theoretical consideration and application. *Eng. Struct.* **2022**, *254*, 113781. [CrossRef]
79. Hawryszków, P.; Biliszczuk, J. Vibration Serviceability of Footbridges Made of the Sustainable and Eco Structural Material: Glued-Laminated Wood. *Materials* **2022**, *15*, 1529. [CrossRef]
80. Karimi, F.; Akbari, R.; Maalek, S. A Simple Conceptual Model for Estimating the First Bending Natural Frequency of Bridge Superstructures. *Shock Vib.* **2022**, *2022*, 1202384. [CrossRef]

Disclaimer/Publisher's Note: The statements, opinions and data contained in all publications are solely those of the individual author(s) and contributor(s) and not of MDPI and/or the editor(s). MDPI and/or the editor(s) disclaim responsibility for any injury to people or property resulting from any ideas, methods, instructions or products referred to in the content.